NOVA IMS Information Management School

MEGI

Master Degree Program in
Statistics and Information Management

Pandemic Bond Pricing: Extending the Hull-White & Stochastic Logistic Growth model with Wang Transform

Insights from Germany Data and Trigger Activation Probability Sensitivity

Mariana Botelho Troufa Real Brandão

Master Thesis

presented as partial requirement for obtaining the Master Degree in Statistics and Information Management

NOVA Information Management School
Instituto Superior de Estatística e Gestão de Informação
Universidade Nova de Lisboa

NOVA Information Management School
Instituto Superior de Estatística e Gestão de Informação
Universidade Nova de Lisboa

Pandemic Bond Pricing: Extending the Hull-White & Stochastic Logistic Growth model with Wang Transform

Insights from Germany Data and Trigger Activation Probability Sensitivity

by

Mariana Botelho Troufa Real Brandão

Master Thesis presented as partial requirement for obtaining the Master's degree in Statistics and Information Management, with a specialization in Risk analysis and management.

Supervised by

Jorge Miguel Bravo, PhD, NOVA Information Management School (NOVA IMS)

March, 2024

STATEMENT OF INTEGRITY

I hereby declare having conducted this academic work with integrity. I confirm that I have not used plagiarism or any form of undue use of information or falsification of results along the process leading to its elaboration. I further declare that I have fully acknowledged the Rules of Conduct and Code of Honor from the NOVA Information Management School.

Mariana Brandão

Lisbon, 14/03/2024

DEDICATION

This achievement is not solely mine. My family's unwavering support and dedication have paved the way for me to reach this moment. I am immensely grateful for their relentless encouragement in both my education and personal growth. To my family, I am proud of each of you and strive to make you proud of the person I am.

None of this would have been possible without the support of my friends, who have become my second family. Your presence has been my solace through every challenge, and I am endlessly thankful for your companionship.

To Bernardo, my best friend who always encourages me to pursue my dreams and has shown unwavering support in my night-owl academic writing process. Thank you for always being by my side.

I want to express my deepest gratitude to my parents. Your endless love, sacrifices, and guidance have been the bedrock of my journey. Thank you for believing in me, for instilling in me the values of hard work and perseverance. This achievement is as much yours as it is mine. I am forever indebted to you both for shaping me into the person I am today.

To my brother, my oldest friend, who has been through thick and thin with me. I wish you all the happiness and success this world has to offer.

And to the one who watches over me from afar, your spirit continues to shape my journey in ways words cannot express. I aspire to embody even a fraction of the person you were.

“ He laughed.” - Kozuki Oden

ABSTRACT

As pandemics show an increasing frequency, research on effective pandemic risk management strategies plays a crucial role in strengthening financial markets and insurance industry resilience to such events. This study proposes an extension for Manathunga and Deng's (2023) pandemic bond pricing framework by integrating the impact of a pandemic inception date relative to the bonds term and adjusting trigger activation probabilities using the Wang transform. As a first approach to pandemic bond pricing using German COVID-19 data, different growth rate scenarios are employed. The following scenarios offer insights into the proposed pandemic bond's price sensitivity relative to possible pandemic start dates and trigger activation probability scenarios. The Wang transform is used to reflect investors aversion or optimism towards pandemic risk from issuance to bonds maturity. This research hopes to contribute to the emerging field of pandemic bond pricing, providing guidance for investors and policymakers navigating pandemic risk in financial markets.

KEYWORDS

Pandemic bonds; Bond valuation; Hull-White model; Stochastic Logistic growth model; Wang transformation; Triggering conditions; Pandemic inception date; Sensitivity analysis; COVID-19.

TABLE OF CONTENTS

LIST OF FIGURES

LIST OF TABLES

LIST OF ABBREVIATIONS AND ACRONYMS

ART	Alternative Risk Transfer
CAT bonds	Catastrophe bonds
COVID-19	Coronavirus Outbreak in 2019
EIOPA	European Insurance and Occupational Pensions Authority
EURIRS	Euro Interest Rate Swap
IDA	International Development Association
ILS	Insurance-linked securities
PEF	Pandemic Emergency Financing facility
ODE	Ordinary Differential Equation
OECD	Organisation for Economic Co-operation and Development
SIR	Susceptible Infected and Recovered
SPV	Special Purpose Vehicle
US	United States
WHO	World Health Organization

1. INTRODUCTION

In 2017 the World Bank issued the first pandemic bonds, designed to transfer pandemic risk from developing countries to global financial markets. These insurance-linked securities followed a catastrophe bond structure, and if certain predetermined catastrophic conditions, or triggers, were met, investors would forfeit the principal invested to cover the losses of the issuer, often an insurance or reinsurance company.

Investors are offered attractive rates for accepting the previously mentioned risk. Although CAT bonds have continuously proven to be an efficient risk transferring mechanism, the latest pandemic bonds were heavily criticized following the COVID-19 pandemic for their inadequate triggers, which were based off the triggers of the first pandemic bond regarding the Ebola pandemic in 2017.

As pandemic occurrences become increasingly more likely, because of global warming and globalization, there arises an urgent need for robust strategies to manage pandemic risk effectively.

1.1. STUDY RELEVANCE AND IMPORTANCE

According to a 2021 OECD report titled "Addressing the Protection Gap for Pandemic Risk: Finding a Way Forward" a variety of social, environmental, and economic factors can lead to more frequent outbreaks of infectious diseases and pandemics. With an increased probability of pandemic outbreaks, effective pandemic bonds play an important role in strengthening financial resilience at individual, industry, and governmental levels as well as contributing to increased public health.

The coronavirus pandemic was the ultimate test for these financial instruments' adequacy, and they have been widely criticized. The complexity behind triggering mechanisms and disbursement requirements revealed in the *Prospectus Supplement* for the World Bank's pandemic bonds, were contributing factors to the bond's inefficiency when facing the 2019 outbreak (*After COVID-19: The Future of Pandemic Bonds*, n.d.).

Piantedosi (2020) highlights the limitations of the existing pandemic bonds, stating "It became clear, unfortunately, that for a virus like COVID-19 the system created by the World Bank is not sufficient to capture in time the evolution of a pandemic; after all, it was constructed on the basis of the Ebola virus, which has a much slower transmission pace, allowing for prompt intervention. A new product should consider this aspect and should try to capture viruses' characteristics into their triggering parameters […] the scientific community aims at finding mechanisms able to predict the frequency of these events."

1.2. THE PRESENT STUDY

In the present study, I extend the existing Hull-White and stochastic logistic growth model pandemic bond pricing framework proposed by Manathunga and Deng (2023) by incorporating a pandemics inception date analysis as well as the Wang transform adjustment to trigger activation probabilities (Wang et al., 2015) accompanied by a comprehensive sensitivity analysis of bond pricing under varying scenarios.

While this methodology prioritizes clarity and accessibility, its important to remain mindful of the inherent limitations, such as the inability to capture term structure dynamics in environments with significant volatility, simplifying assumptions, and its sensitivity to calibration instrument choice, which could lead to model misspecification.

Multi-factor models are stronger tools for capturing interest rate dynamics than the chosen one-factor Hull-White model. Ultimately, the model choice aligns with the desired balance between implementation ease, which leads to a better understanding of its results, and an accurate depiction of future interest rates for the purposes of this study. As for the stochastic logistic growth model choice, it has demonstrated effectiveness in estimating death and infection COVID-19 cases (Otunuga and Otunuga, 2022; Shen, 2020; Triambak et al., 2021). Its innovative application for pandemic bond pricing in 2023 also sparked interest, prompting its inclusion in this study. Furthermore, the introduction of the Wang transform in this context allows for a more nuanced understanding of bond pricing under varying lambda parameters.

While Manathunga and Deng (2023) calibrate their model to US COVID-19 data, I will focus on a numerical approach to pricing the proposed pandemic bonds using Germany COVID-19 data. This decision was driven by the country's strong healthcare infrastructure and policy responses, which may differ from those of the United States.

As the literature on pandemic bond pricing remains limited, this study aims at further exploring this new and emerging field and contributing with valuable insights to the sensitivity of pandemic bond prices to pandemic start date relative to the bonds' term and trigger activation probabilities.

2. LITERATURE REVIEW

The CAT bond market emerged in 1997, prompted by the impact of Hurricane Andrew in 1992. Its growth has been influenced by major events such as Hurricane Katrina in 2005, the financial crisis of 2008, and the subsequent low-interest-rate period (Polacek, 2018). Furthermore, high reinsurance prices following the $62 billion insured losses due to Hurricane Katrina attracted investors to the CAT bond market as a means of diversifying risk in their portfolio (Polacek, 2018).

Throughout the last decade, the catastrophe bond market has registered substantial growth. In the fourth quarter of 2023, the catastrophe bond, and insurance-linked securities (ILS) market experienced unprecedented activity, marking the busiest fourth quarter in its history (Artemis, 2024; Holzheu et al., 2023). The Artemis "Q4 2023 Catastrophe Bond & ILS Market Report" highlights $5.6 billion of issuance across full 144A CAT bond transactions (144A refers to the resale of securities, not their initial issuance), CAT bonds covering non-catastrophic risks, such as cyber and mortality, and privately placed deals. According to Artemis, it is the fifth time quarterly issuance has exceeded $5 billion. The average size of transactions increased by 27% with an average price change of issuance at +2.7%. Data shows that the average size of issuance during the fourth quarter of 2023 is around $168 million, approximately 61,9% higher than in the previous year (Artemis, 2024). The overall catastrophe bond market size grew by 19% reaching $45 billion in 2023, highlighting robust investor appetite and favorable market conditions as there is growing demand for catastrophic risk transfer mechanisms (Holzheu et al., 2023).

According to Braun (2012), despite the growing importance of catastrophe bonds visible in 2012, there were limited scholarly resources on the pricing of CAT bonds, which remains true today.

2.1. CATASTROPHE BONDS

Catastrophe bonds are insurance-linked securities designed to address high-severity, low-probability events. These debt instruments with elevated yields aim to provide supplementary funding to insurers and reinsurers in the event of a natural disaster, like an earthquake or a hurricane (European Insurance and Occupational Pensions Authority [EIOPA], 2021). Risks arising from natural catastrophes are ceded to investors through a Special Purpose Vehicle (SPV), responsible for bond issuance and reinvesting its proceeds, raising funds for potential payouts should triggering conditions be met. Similarly to regular corporate bonds, if no catastrophe occurs investors receive coupon payments and the principal amount at maturity (Piantedosi, 2020). Figure 1 displays an illustrative structure behind a catastrophe bond transaction.

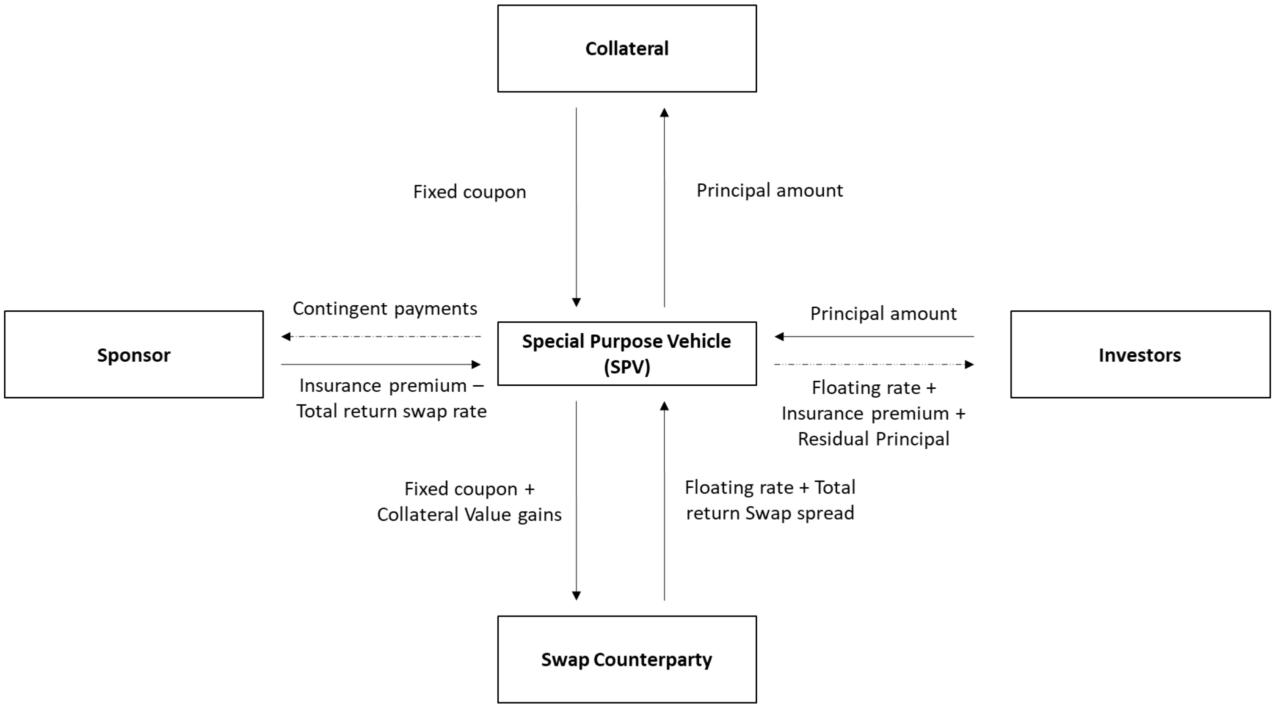

Figure 1: Structure of a catastrophe bond transaction.

In a catastrophe bonds' structure, the sponsor, typically an insurer or reinsurer, initiates catastrophe bond issuance to transfer some of its catastrophic risk to capital markets. As depicted in Figure 1, a special purpose vehicle (SPV) serves as an intermediary between sponsor and investors, holding bond proceeds in a trust account (collateral). The SPV is also responsible for distributing coupon payments and principal amount to investors, according to the bonds established payout structure. The collateral is usually invested in low-risk assets such as government securities. In some catastrophe bond structures, a swap counterparty may be involved, providing additional protection to the sponsor by taking on some risks, such as interest rate risk. The swap counterparty receives fixed coupon payments from the SPV and may benefit from a potential increase in collateral valuation (Braun, 2012).

Before delving into the existing literature on the pricing of catastrophe bonds, I will introduce some general concepts and notions, such as market incompleteness and an affine term structure. The catastrophe bond market is typically considered incomplete, stemming from traditional hedging mechanisms' inability to provide full protection against catastrophic risks, due to the unique and unpredictable nature of the events that characterize them. The affine term structure model allows for a systematic approach to incorporating interest rate dynamics into the pricing of catastrophe bonds and a clearer understanding of the relation between payouts and the term structure of interest rates in this context.

2.1.1. CAT Bond pricing methodologies

This literature review on catastrophe bond pricing will be structured by distinguishing between methodologies that align with two main theories outlined by Braun (2012): option pricing theory and equilibrium pricing theory.

Option pricing theory consists of approaching catastrophe bonds as contingent claims on future catastrophic events and assumes market completeness, while equilibrium pricing theory accounts for market dynamics and investor behaviour in both complete and incomplete market settings.

Firstly, I will present an overview of the literature focusing on catastrophe bond valuation methodologies derived from option pricing theory. Lee and Yu (2002) incorporate the square-root short rate process (Cox et al., 1985) and account for stochastic interest rates, moral hazard, basis risk and default risk in their contingent claim approach to pricing default-risky catastrophe bonds, ultimately demonstrating the link between moral hazard and basis risk and a downward trend on bond prices. Vaugirard (2004; 2003a; 2003b) assumes stochastic interest rates under the Vasicek (1977) model and introduces a payoff structure for catastrophe bonds dependent on an underlying index and a defined threshold (similarly to barrier options). The underlying physical index is modeled by a jump-diffusion process. By incorporating sudden discontinuous jumps in addition to continuous random movements (diffusion), the author allows for a more flexible and realistic approach to the underlying risk affecting the price of the ILS. Burnecki and Kukla (2003) present a compound doubly stochastic Poisson model and derive non-arbitrage prices for zero-coupon and coupon catastrophe bonds, calibrating the model to 10-year catastrophe loss data by Property Claim Services.

Härdle and Cabrera (2010) calibrated a pure parametric catastrophe bond to Mexican earthquake data gathered from the National Institute of Seismology in Mexico. The chosen triggering event was the magnitude of the earthquakes exceeding a predefined threshold. The authors price the bond through a compound doubly stochastic Poisson process methodology (Burnecki and Kukla, 2003) while acknowledging that this methodology is typically used for index triggers.

Jarrow (2010) proposes a simple closed form solution for valuing catastrophe bonds consistent with an arbitrage-free model, derived from reduced form models for credit derivatives pricing (see: Jarrow, 2009). Ma and Ma (2013) extended the contingent claim model developed by Lee and Yu (2002) by incorporating a compound nonhomogeneous Poisson loss process. While a homogenous Poisson process is characterized by constant catastrophic event intensity, a nonhomogeneous Poisson process allows for a more realistic approach to the severity of catastrophic events over time. Furthermore, the compound doubly stochastic Poisson adds another stochastic dimension to pricing, as the intensity of catastrophic events itself follows a stochastic process. The compound aspect of the model reflects the collective impact of multiple catastrophic events on overall losses.

Faced with catastrophe bond pricing under an incomplete market setting, authors resort to equilibrium pricing theory. Cox and Pedersen (2000) explored equilibrium pricing theory through a two-stage approach consisting of estimating the interest rate process in the absence of a catastrophic event and then incorporating these estimates with the probability of a catastrophe occurring when pricing the financial instruments. A potential disadvantage of this foundational work on the pricing of catastrophe bonds lies in its simplicity as it may not represent the full complexity of market dynamics. Additionally, Young (2004) explored the principle of equivalent utility when computing indifference prices within an incomplete market setting, along with the integration of an affine term structure model. The author priced a catastrophe risk bond considering an exponential utility function for investor preferences and derived a partial differential equation for the indifference prices that resembles the Black-Scholes equation with a nonlinear term reflecting the writers risk aversion in an incomplete market. Egami and Young (2007) extend Young's (2004) research by applying the utility indifference pricing methodology to *structured* catastrophe bonds issued in two distinct notes (a junior and a senior tranche with unique payment schedules).

Finally, Deng et al. (2020) introduced a novel application of catastrophe bond pricing models to drought catastrophe risk on a global scale. The authors develop a “Peak over threshold” model to estimate tail risk, an approach based on extreme value theory.

2.2. Pandemic Bonds

Pandemics are a category of CAT bonds, where the insured risk is the risk of a global outbreak of a contagious disease. Pandemic bond proceeds are intended for disbursement to countries or regions affected by the designated health emergency. Pandemic risk differs from other types of catastrophe risks, such as hurricanes, earthquakes, and wildfires, which are routinely underwritten by insurers and reinsurers. Damages arising from natural catastrophes generally occur within a short period of time and its effects dissipate over the span of hours or days and impact a limited number of policyholders. Due to this, these events rarely have systemic impacts on financial markets. Conversely, pandemics impact nearly all policyholders and have extended losses for a span of months or years, which prevents risk pooling and diversification, not allowing for loss redistribution. In fact, the COVID-19 outbreak established a correlation between losses arising from the pandemic, financial markets, and other insurance losses. During the first months of 2020, the surplus held by U.S. property-casualty insurance companies decreased significantly, due to a sharp decline in asset prices and the creation of COVID-19 loss provisions across insurance lines (Hartwig et al., 2020).

2.2.1. Pandemic Bond pricing methodologies

Pandemic bonds are being actively considered in various proposals for future insurance schemes, particularly in response to the COVID-19 pandemic (EIOPA, 2021). Additionally, discussions around Alternative Risk Transfer (ART) and Insurance-Linked Securities (ILS) have also brought to light pandemic bonds, reflecting the ongoing interest in leveraging pandemic bonds as a means of transferring and managing pandemic-related risks within the insurance and financial sectors.

Despite the recent boost in the catastrophe bond market, namely in mortality catastrophe bonds, the existing literature on pandemic bond pricing is limited. Fan and Mamon (2023) introduce a novel approach to assessing pandemic emergency financing facilities. The authors integrate the Susceptible-Infected-Removed (SIR) compartmental model with a Vasicek interest rate process (Vasicek, 1977) evaluating bond prices under different scenarios through Monte Carlo simulation. The researchers use Canadian COVID-19 data to assess the performance of the stochastic SIR-Vasicek model, providing empirical insights on bond payouts in case of a pandemic. Huang et al. (2021) provide a comprehensive analysis on pandemic bonds and endemic swaps and introduce novel structures for these instruments, namely binary coupon and fixed or binary principal structures. Empirical analysis of the pricing of the proposed coronavirus pandemic bond was computed on the expected discounted cashflows based on the equivalent martingale measure.

Chen et al. (2022) propose a mortality model that considers both country-specific mortality shocks and pandemic mortality shocks in an article titled “Modeling pandemic mortality risk and its application to mortality-linked security pricing”. The article presents a threshold jump approach to modeling pandemic mortality risk, which considers the sudden increase in mortality rates during pandemics and provides a framework for analyzing the effects across different countries. The authors explore an analytical solution for pricing mortality-linked securities, derived through the Wang transform (C. W. Wang et al., 2015) and the Denuit et al. (2007) approach. Zheng and Mamon (2023) evaluate the World Bank's pandemic bond (World Bank, 2017b) pricing framework and triggering conditions. The authors recommend a substantial reduction of triggering conditions, as simpler triggering mechanisms result in quicker aid to countries in need. Li et al. (2023) present a comprehensive analysis on pricing extreme mortality risk in a global health crisis. The authors describe the joint interest rate and excess mortality dynamics with a bivariate jump-diffusion model. They highlight a significant negative correlation between interest rates and excess mortality for recent US data, as well as a heightened jump intensity during the COVID-19 pandemic. The impact of shifts in excess mortality on interest rates contrasts with the previous assumption of independence between the catastrophic event and the financial markets, advocating for further research for future pandemic bond issuance.

Moreover, recent advancements in mortality modelling have prompted innovative approaches to pandemic bond pricing. For instance, Manathunga and Deng (2023) propose a novel pandemic bond pricing framework based on the Hull-White interest rate model (Hull and White, 1990) and the stochastic logistic growth model (Khodabin et al., 2012; Liu & Wang, 2013). Previous studies have mostly focused on SIR models, but stochastic logistic models have proven efficient in death and infected cases estimation for COVID-19 data (Otunuga and Otunuga, 2022; Shen, 2020; Triambak et al., 2021).

2.2.2. World Bank and the first pandemic bond

Following the Ebola outbreak in West Africa, the World Bank designed a rapid response financing mechanism for developing countries when facing a large-scale outbreak, the Pandemic Emergency Financing facility (PEF) (World Bank, 2017a). The pioneer initiative addressed pandemic risk through two components: the insurance and the cash windows.

Figure 2 illustrates the structure behind the first pandemic bond as well as PEF's insurance window.

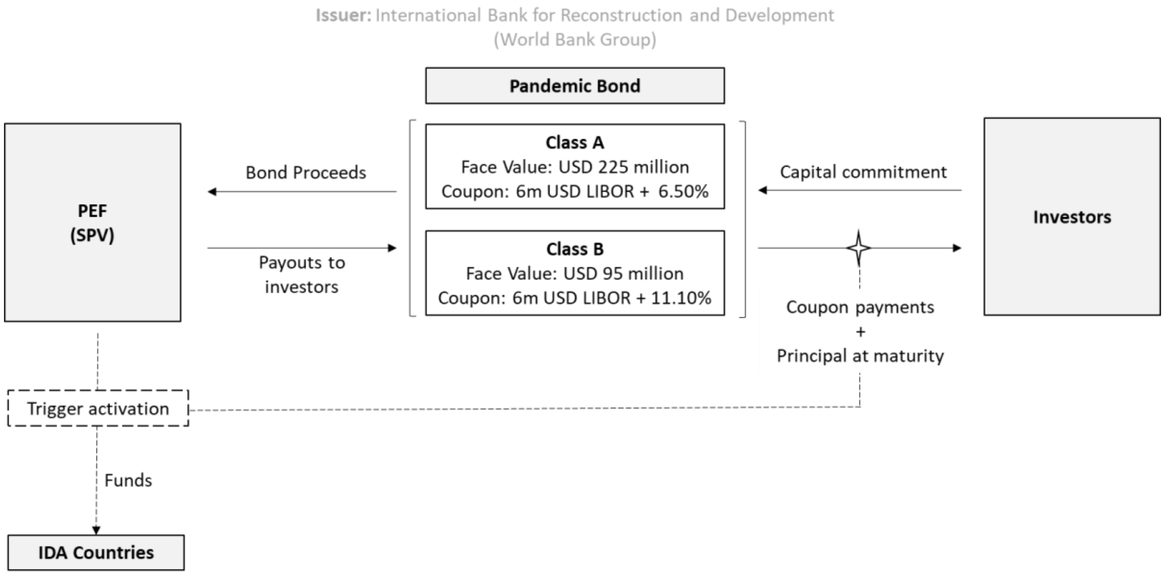

Figure 2: Structure of World Bank's first pandemic bond and PEF's Insurance window.

The insurance window was funded by Japan and Germany, in close collaboration with Swiss Re and Munich Re, offering protection against a cross-border disease outbreaks for some of the poorest countries in the world(World Bank, 2017b). The PEF aimed at providing more than US$500 million in protection against pandemic outbreaks in IDA countries over a period of five years. The bonds covered six high-risk virus groups through two bond classes, A and B(World Bank, 2017b). The insurance window enabled market participants to play a role in this regard. Should triggering conditions for the bonds be met, bond proceeds as well as future coupon payments to investors would be disbursed to PEF beneficiaries, as depicted in Figure 2. The pandemic bond's triggering conditions, such as certain levels of contagion, mortality rate and the declaration of a pandemic outbreak by the World Health Organization (WHO), resulted in investors forfeiting the invested principal to cover the losses of the issuer. The cash window provided additional funding outside the insurance window, providing a faster funding mechanism (Zheng & Mamon, 2023).

2.3. Limitations

The Financial Times, in collaboration with Calvert, published an article titled "After COVID-19: The Future of Pandemic Bonds" where the limitations of the World Bank's first pandemic bond when facing the COVID-19 health crisis are discussed. High complexity of trigger conditions, extended waiting periods, limited impact, and difficulties in principal risk evaluation have also been discussed in detail by Zheng and Mamon (2023). The following limitations can be highlighted:

1. The bonds required a waiting period of 12 weeks following the "event date" of a pandemic, followed by additional weeks for data analysis and an arbitrator's determination, before funds could be released.
2. The complexity and rigidity of the bond's trigger conditions resulted in delayed disbursement of proceeds and funds to countries in need during the COVID-19 pandemic, defeating the set-out goal for the financial instrument, which consisted in providing timely support to countries at risk.

3. The extensive nature of the *prospectus* and the complexity of the trigger mechanisms have posed difficulties for investors in comprehending the precise terms and conditions of the bonds, which posed challenges regarding principal risk assessment.

3. METHODOLOGY

3.1. INTEREST RATE SIMULATION USING HULL-WHITE MODEL

The one-factor short-rate Hull-White model extension (Hull and White, 1994) will be used to predict interest rate dynamics over time. The Hull-White model extends the (Vasicek, 1977) by incorporating a time-varying mean reversion and the market forward rate curve (Kladívko and Rusý, 2023).

3.1.1. Relevant Notation

Following Kladívko and Rusý (2023) , let $P(t, T)$ denote the price of a zero-coupon bond at time t with a single notional principal amount disbursed at maturity (T). The continuously compounded yield at time t is given as:

$$y(t,T) = -\frac{\ln P(t,T)}{T-t}, \qquad t \leq T \tag{1}$$

The forward rate established at time c for the upcoming time period $[t, T]$ is defined by:

$$f(c,t,T) = -\frac{\ln P(t,T)}{(T-t)P(c,T)}, \qquad c \leq t \leq T \tag{2}$$

The instantaneous forward curve at time c , denoted as $f(c,\cdot) \coloneqq \{f(c,T),\ c \leq T\}$, represents the set of instantaneous forward rates maturing at time T observed at time c, defined as:

$$f(c,t) \coloneqq \lim_{T \to t^+} f(c,t,T) - \frac{\partial \ln P(c,t)}{\partial t}, \qquad c \leq t \leq T \tag{3}$$

The short rate is set as $r(t) := f(t,t)$.

3.1.2. The Hull-White model

Under the risk-neutral measure, the one-factor Hull-White short rate process is given by the following stochastic differential equation (SDE):

$$dr_c(t) = \big(\theta_c(t) - \alpha_c r(t)\big)dt + \sigma dB(t), \qquad c \leq t \tag{4}$$

Where c denotes the calibration time for the model parameters, $r_c(t) = f^M(c,c)$ the short rate, is the instantaneous market forward rate at time c, $\theta_c(t)$ denotes the mean reversion function, α_c the mean reversion speed, σ is the volatility parameter, and $B(t)$ is the standard Brownian motion under the risk-neutral measure.

$$\theta_c(t) = \frac{\partial f^M(c,t)}{\partial t} + \alpha_c f^M(c,t) + \frac{\sigma^2}{2\alpha_c}\big(1 - e^{-2\alpha_c(t-c)}\big), \qquad c \leq t \tag{5}$$

Where $f^M(c,t)$ is the observed market forward rate at time $c \leq t$. The Hull-White zero-coupon bond pricing function is defined as (see appendix B: Kladívko and Rusý, 2023):

$$P_c(t,T) = e^{A_c(t,T) - B(t,T) r_c(t)} \tag{6}$$

Where,

$$B(t,T) = \frac{1 - e^{-\alpha(T-t)}}{\alpha}, \tag{7}$$

$$A_c(t,T) = f^M(c,t,T)(T-t) + B(t,T)f^M(c,t) - B(t,T)^2 \frac{\sigma^2}{4\alpha_c}\left(1 - e^{-2\alpha_c(t-c)}\right) \tag{8}$$

The numerical implementation of the Hull-White model in this study relies on an underlying linear interpolation method for short rate estimation, as well as a constant mean reversion speed function and a piecewise constant volatility function calibrated using appropriate instruments, defined as follows (Lee, 2021).

$$\sigma(t) = \begin{cases} \sigma_1, & t_0 \le t \le t_1 \\ \sigma_2, & t_1 < t \le t_2 \\ & \dots \\ \sigma_{T-1}, & t_{T-2} < t \le t_{T-1} \\ \sigma_T, & t_{T-1} < t \le t_T \end{cases} \tag{9}$$

Where T is the specified maturity for the bond in valuation. This allows for a more flexible approach to estimating interest rates compared to a single constant volatility parameter.

Other interpolation methods, such as the cubic spline interpolation or polynomial interpolation methods, could have been used, but the linear interpolation method provides the desired trade-off between accuracy and computational efficiency for this study. The model also assumes independence between pandemic risks and financial markets, which can be argued following COVID-19 pandemic (Hartwig et al., 2020).

3.2. Trigger Activation Modeling with Stochastic Logistic Growth Model

3.2.1. Assessing Pandemic Risk

Consider the events defined in Table 1:

Table 1: Event definition for pandemic risk evaluation

$\boldsymbol{H}$:= Occurrence of a pandemic
$\boldsymbol{H'}$:= Absence of a pandemic event
$\boldsymbol{C}$:= Bond triggering conditions are activated
$\boldsymbol{C'}$: = Bond triggering conditions are not met

By the law of total probability,

$$\mathbb{P}(C) = \mathbb{P}(C|H)\mathbb{P}(H) + \mathbb{P}(C|H')\mathbb{P}(H') \tag{10}$$

$$\mathbb{P}(C') = \mathbb{P}(C'|H)\mathbb{P}(H) + \mathbb{P}(C'|H')\mathbb{P}(H') \tag{11}$$

It is assumed that there is no possibility of trigger activation under a scenario where a pandemic event has not occurred, thus $\mathbb{P}(C \mid H') = 0$. Additionally, note that $\mathbb{P}(C) + \mathbb{P}(C') = 1$. The pandemic bond will be valued under the following probabilities regarding trigger activation:

$$\mathbb{P}(C) = \mathbb{P}(C|H)\mathbb{P}(H) \tag{12}$$

$$\mathbb{P}(C') = 1 - \mathbb{P}(C) \tag{13}$$

I follow the approach suggested by Fan and Mamon (2023) and assume $H \sim Poisson(\lambda)$ to calculate the probability of pandemic occurrences during the pandemic bond's term. Let n denote the number of pandemic events for the period in scope, denoted by T_{period} in years, and T the bond maturity expressed in years, then:

$$\lambda = \left(\frac{nT}{T_{period}}\right) \tag{14}$$

$$\mathbb{P}(H') = e^{-\lambda} \tag{15}$$

$$\mathbb{P}(H) = 1 - e^{-\lambda} \tag{16}$$

3.2.2. Stochastic Logistic Growth Model Overview

The logistic function was originally devised by the Belgian mathematician Verhlust (Vogels et al., 1975), and the logistic growth model has emerged in recent years regarding the COVID-19 pandemic (Shen, 2020; Triambak et al., 2021). The model is described by the following Verhlust ordinary differential equation (ODE):

$$\frac{dN(t)}{dt} = gN\left(1 - \frac{N(t)}{K}\right) \tag{17}$$

Where, $N(t)$ represents population size at time t, g is the intrinsic growth constant and K denotes the carrying capacity, which is the asymptotic limit for $N(t)$ as $t \to +\infty$ (for $g \neq 0$). The stable equilibrium points for Equation (17) are 0 (unstable equilibrium) and K(stable equilibrium)(Liu and Wang, 2013) and the solution to the ODE is of the form:

$$N(t) = gN\left(1 - \frac{K}{1 + ae^{-gt}}\right) \tag{18}$$

Where $a = \frac{K-N(0)}{N(0)}$.

Liu and Wang (2013) addressed the concept of time-varying growth rates influenced by environmental noise in the logistic growth model, revealing that white noise is unfavorable for the stability of the positive equilibrium (K) in the logistic equation. This approach allows for a more comprehensive framework that captures the complexity of a real-world scenario for population growth (as populations do not typically grow at a constant rate) as well as the unpredictability of the population's environment, particularly in the context of pandemic modelling. The environmental noise is introduced into the logistic model through a stochastic differential term $\sigma(t)dB(t)$.

$$g \rightarrow g(t) + \sigma(t)dB(t)$$

Where, $\sigma(t)$ is a function that represents the intensity of random fluctuations (white noise) affecting the growth rate $g(t)$ and $dB(t)$ is the differential of a standard Brownian motion process, which is a continuous-time stochastic process with independent and normally distributed increments. If $\sigma(t)$ and

$r(t)$ are bounded[1] and continuous[2] functions on $[0, \infty)$. By applying this modification, we derive the following stochastic nonautonomous logistic equation[3](Liu and Wang, 2013):

$$dN(t) = N(t)\left(1 - \frac{N(t)}{K}\right)\big(g(t)dt + \sigma(t)dB(t)\big) \tag{19}$$

Through Itô calculus, the solution for the stochastic nonautonomous logistic equation is as follows (Liu and Wang, 2013):

$$N(t) = \frac{K}{1 + \left(\frac{K}{N(0)} - 1\right) e^{-\int_0^t \left(g(s) - \frac{\sigma^2(s)N(s)}{2} - \frac{\sigma^2(s)N(s)}{K}\right)ds - \int_0^t \sigma(s)dB(s)ds}} \tag{20}$$

If $0 < N(0) < K$, the stability of the equilibrium points of the stochastic nonautonomous logistic equation is given by (see Theorem 1, Liu and Wang, 2013):

1. The 0 solution is globally asymptotically stable a.s. (almost surely) if

$$\lim_{t\to\infty} \sup t^{-1} \int_0^t g(s) \; - \frac{\sigma^2(s)}{2} ds < 0 \tag{21}$$

1. The positive equilibrium solution K is globally asymptotically stable a.s. if

$$\lim_{t\to\infty} \inf t^{-1} \int_0^t g(s) \; - \frac{\sigma^2(s)}{2} ds > 0 \tag{22}$$

The stability conditions in Equations (21) and (22) are noted to be weaker when compared to those of previous studies (Golec and Sathananthan, 2003), shedding light on the nuances of stability in stochastic growth models (Liu and Wang, 2013). The presence of white noise in the system is unfavorable for the stability of the positive equilibrium solution K, which suggests that the randomness that is introduced in the logistic model prevents the population growth from stabilizing at the carrying capacity.

The stochastic logistic growth model is applied to the number of infected cases, denoted as $I(t)$, and the number of deaths, denoted as $D(t)$, at time t for a pandemic occurrence. For numerical implementation ease and result interpretability, constant growth rate and volatility functions will be used, therefore, the infected and deaths processes are described as:

---

[1] A function $f(t)$ is said to be a bounded function if

$$\exists M < \infty \,, \forall t \in [0, \infty) : \; |f(t)| \leq M$$

[2] A function $f(t)$ is said to be a continuous on $[0, \infty)$ if

$$\forall \varepsilon > 0 \,, \exists \delta > 0 : \forall t_1, t_2 \in [0, \infty) \,, |t_2 - t_1| < \delta \Longrightarrow |f(t_2) - f(t_1)| < \varepsilon$$

[3] A nonautonomous logistic equation is a mathematical model for describing population growth over time. Nonautonomous refers to a mathematical equation (or system) whose behavior explicitly depends on an external parameter, such as time or another independent variable. The deterministic part of the equation captures the logistic population growth dynamics over time and the stochasticity refers to the randomness term of the equation.

$$dI(t) = I(t)\left(1 - \frac{I(t)}{K_I}\right)\left(g_I dt + \sigma_I dB_I(t)\right) \tag{23}$$

$$dD(t) = D(t)\left(1 - \frac{D(t)}{K_D}\right)\left(g_D dt + \sigma_D dB_D(t)\right) \tag{24}$$

Where g_I and g_D denote the constant growth rates for infected and deaths and σ_I and σ_D the constant volatility for infected and death growth rates, respectively. A correlation of $\rho_{I,D}$ is assumed to exist between the number of infected and dead (Manathunga and Deng, 2023). Thus,

$$dB_I(t) = dW_1(t) \tag{25}$$

$$dB_D(t) = \rho_{I,D} dW_1(t) + \sqrt{1 - {\rho_{I,D}}^2} dW_2(t) \tag{26}$$

Where $W_1(t)$ and $W_2(t)$ are two independent standard Brownian motions. Note that a nonautonomous approach to this correlation would lead to more accurate depictions, as the correlation between dead and infected may relate to time. As an example, for periods with a high number of infected and significant growth rate, the healthcare system may be under too much pressure and malfunction, hospital can become overwhelmed by the number of infected, leading to poorer conditions and ultimately a higher number of deaths.

3.2.3. Trigger Activation Probability Modeling

The probability of trigger activation under a pandemic scenario will be empirically derived under Monte Carlo simulation methods for the stochastic logistic growth processes, and is given as:

$$\mathbb{P}(C|H) = \frac{Number\ of\ simulated\ paths\ with\ trigger\ activation}{Total\ number\ of\ simulated\ paths} \tag{27}$$

3.3. Wang-Transform Adjustment of Trigger Activation Probability Distribution

Wang (2000) introduced a new class of distortion operators $p_\lambda: [0,1] \rightarrow [0,1]$ defined as:

$$p_\lambda(u) = \phi[\phi^{-1}(u) + \lambda], \qquad \lambda \in \mathbb{R} \tag{28}$$

Where ϕ is the standard normal cumulative distribution, that is $\phi(x) = \int_0^x \frac{1}{\sqrt{2\pi}} e^{-\left(\frac{1}{2}\right)s^2} ds$.

Parameter λ can be seen as the market price of risk (Labuschagne and Offwood, 2013), representing the markets' level of risk aversion optimism regarding the occurrence of triggers and their impact on the bond's payouts. A sensitivity analysis on the λ parameter allows for the incorporation of market risk preferences on the pricing and assessment of triggering events in pandemic bond valuation.

Let $F_X(x)$ denote the probability distribution for triggering events to be met on a certain day. $p_\lambda\left(F_X(x)\right)$ defines a distorted probability distribution for triggering event occurrence relative to the bonds term, whose mean yields a risk-adjusted trigger activation probability that allows for the incorporation of the market price of risk on bond valuation given the perceived impact of the triggering events timeline (Wang, 2000).

Previous authors have acknowledged the limitations of the original Wang transform in comparison with extended models, as it relies on normal distributions and may not adequately depict fatter tails observed in actual markets. Kijima and Muromachi (2008) suggest using Student's t distribution with a higher degree of freedom for a more accurate model on financial and insurance asset returns. Additionally, the authors discuss the two-parameter Wang transformation, reflecting how this approach yields more accurate depictions of market prices, but ultimately lacks economic interpretability due to inconsistencies with Bühlmann's economic premium principal (see: Bühlmann, 1980; Kijima and Muromachi, 2008).

3.4. PRICING MODEL

3.4.1. Triggering conditions

Triggering conditions are crucial determinants in pandemic bond valuation, as the payout structure for these financial instruments is dependent on trigger activation. The World bank's first pandemic bond was criticized for the complexity of cumulative triggering conditions stated in the bonds Supplemental Prospectus (2017), as it was meant to provide efficient aid to third-world countries, however too lenient triggering conditions pose drawbacks from an investor's perspective, as the likelihood of coupon and principal amount losses would inevitably increase. Therefore, the triggering conditions chosen for the purposes of this study aim at providing a balanced approach between trigger complexity and efficacy for these instruments. The following triggering conditions were established by Manathunga and Deng (2023) and will be used as a foundation for this study:

1. The seven-day moving average for daily new infected, $MA_I(t)$, must exceed θ_I
2. The seven-day moving average for daily new deaths, $MA_D(t)$, must exceed θ_D
3. The outbreaks growth rate, $G(t)$, must be positive. The growth rate is defined as
$$G(t) = MA_I(t) - 1.5333\sigma_I(t) \tag{29}$$
Where $\sigma_I(t)$ is the standard deviation of new infected cases for the past week.

The thresholds for infections, θ_I, must exceed 1% and the threshold for deaths ,θ_D, must exceed $0{,}005\%$ of the population for the country or region in scope. This approach allows for a more realistic approach to triggering conditions and the percentages can be adjusted to reflect a country's health regulations.

Consequently, the trigger time is set as:

$$\tau = \inf\{t \mid MA_I(t) > \theta_I \wedge MA_D(t) > \theta_D \wedge G(t) > 0\} \tag{30}$$

3.4.2. Payout structure

Consider a pandemic bond maturing at time T with n coupon payments $C_{t_1}, C_{t_2}, \dots, C_{t_n}$ dependent on a floating rate and occurring at times $t_1, t_2, \dots, t_n$ with a face value FV. The payout structure for the proposed pandemic bond is:

$$Payout_{total} = \begin{cases} \sum_{i=1}^{k} C_{t_i}, & t_k < \tau < t_{k+1} \leq T \\ FV + \sum_{i=1}^{n} C_{t_i}, & \tau \geq T \end{cases} \tag{31}$$

If triggering conditions are met, the investor receives all expected coupon payments up to that date, forfeiting future coupon payments and redemption amount, FV. On the other hand, if bond triggering conditions are not met during the bond's term, the bondholder will receive all coupon payments as well as the principal amount, FV, at maturity.

3.4.3. Pricing

Cox and Pedersen (2000) acknowledge an incomplete market setting when pricing catastrophe bonds, as the payoffs for these instruments cannot be hedged by traditional securities. The authors underscore the weaker interpretability of the pricing of uncertain cash flows in comparison to a market completeness framework, highlighting how relevant the investors attitude towards risk in an incomplete market setting. As there is no consensus in a pricing framework for pandemic bonds, the pricing methodology adopted in this study aligns with those of previous authors (Manathunga and Deng, 2023). The pricing approach adopted in this study integrates the previously defined models and relies on Monte Carlo simulation methods to compute the bonds expected price across all simulations. The pricing methodology is discussed in detail below.

Consider the bonds maturity T, the face value FV, the coupon payment dates relative to the bonds term, $t_1, t_2, \ldots, t_T$, the predicted average coupon rates from the Hull-White model simulated interest rate paths r_{t_1}, r_{t_2}, ..., r_{t_T} and discount factors DF_{t_1}, DF_{t_2}, ..., DF_{t_T}. Coupon payment amounts are computed as:

$$C_{t_i} = FV \times r_{t_i}, \qquad t_i \in [0, T] \tag{32}$$

As a result, the present value of each cash flow is given as:

$$PVCF_{t_i} = C_{t_i} \times DF_{t_i}, \qquad t_i \in [0, T) \tag{33}$$

$$PVCF_{t_T} = (C_{t_T} + FV) \times DF_{t_T} \tag{34}$$

Thus, the bonds present value accounting only for interest rate risk is:

$$PV = \sum_{i=1}^{T} PVCF_{t_i}, \qquad t_i \in [0, T] \tag{35}$$

Consider the simulation of J pandemic paths through the stochastic logistic growth model described in Equations (23) and (24). Let H_j denote the j-th pandemic event simulated by the model, associated with a trigger activation time τ_j. By integrating the Hull-White's model predictions with the stochastic logistic growth model's pandemic event H_j the expected bond price, P_{H_j}, under that pandemic scenario is given as:

$$E\left[P_{H_j} \mid H_j\right] = \begin{cases} \sum_{i=1}^{k} PVCF_{t_i}, & t_k < \tau_j < t_{k+1} \leq T \\ \sum_{i=1}^{T} PVCF_{t_i}, & \tau_j > T \end{cases} \tag{36}$$

The expected bond value given a pandemic event during the bonds term, $E[P_H \mid H]$, is calculated as the average of all expected bond prices across the triggered simulations.

Let C denote a triggering event. The probability of a pandemic occurring during the bonds term, $\mathbb{P}(H)$, given by Equation (16), and the probability of a triggering event, $\mathbb{P}(C)$, is given in Equation (12), where $\mathbb{P}(C|H)$ is the number of simulated pandemic paths divided by the number of simulations J, like depicted in Equation (27). Overall, the fair value for the pandemic bond is computed as follows,

$$P = E[P_H \mid H]\mathbb{P}(C) + E[P_{H'} \mid H']\mathbb{P}(C') \tag{37}$$

Where $E[P_{H'} \mid H']$ denotes the bonds present value in the absence of a triggering event, calculated using Equation (35).

4. RESULTS AND DISCUSSION

This study focuses on numerically simulating the fair price for a three-year maturity pandemic bond. The interest rate process is modelled using the Hull-White model calibrated to Euribor and Euro interest rate swap (EURIRS) yields. The stochastic logistic growth model plays a pivotal role in the adopted pricing methodology, as bond payouts are contingent on pandemic events. This model is calibrated to COVID-19 data specific to Germany. This analysis relies on the characteristics of the proposed bond, specifications of the interest rate model, the probability of a pandemic occurring, and the likelihood of trigger activation. Numerical implementation for the interest rate model and the pandemic growth model will be conducted through Monte Carlo simulation methods using R programming (R Core Team, 2023), leveraging the R codes proposed by Lee (2021) and Manathunga (2023).

Additionally, I discuss results for different pandemic scenarios and their impact on bond valuation as well as conduct a sensitivity analysis of bond prices to the pandemic start date and trigger activation probabilities using the Wang transform.

4.1. BOND CHARACTERISTICS

Issued on 01/01/2024 and maturing on 01/01/2027, the proposed pandemic bond has a face value of 200 million EUR and will be valued under the Actual/360-day convention. Should triggering conditions be met, investors lose all future coupon payments and principal amount at maturity. Conversely, in the absence of a triggering event, investors can expect semi-annual floating coupons at the Euribor rate with a tenor of six months plus a 650 basis points spread.

Future Euribor 6-months rates will be predicted under the Hull-White model calibrated as of 31/12/2023 using Euro Interest Rate Swap historical data. The catastrophic risk is accounted for under the stochastic logistic growth model calibrated using COVID-19 data for Germany.

Table 2: Interest rate model parameters

Bond parameters	
Issuance date	01/01/2024
Settlement date	01/01/2024
Maturity date	01/01/2027
Term	3 Years
Face value	EUR 200 M
Coupon rate	E6M + 650BPS
Payment date	Semi-annual payments on the first day of each semester
Day convention	Actual/360
Hull-White model	Calibrated on 31/12/2023
Stochastic-logistic growth model	Calibrated using Covid-19 data for Germany

4.2. HULL-WHITE MODEL SIMULATION AND BOND VALUATION

Kladívko and Rusý (2023) suggested a maximum likelihood method to estimate the Hull–White model, calibrating the model on various time series of EUR yields. Similarly, I calibrated the Hull-White one-factor model using EUR interest rate swap daily historical data and monthly Euribor rates historical data, retrieved from Investing.com (n.d.) and EURIBOR.EU (n.d.).

The use of cross-sectional data from a single point in time allows for a perfect fit of the market yield curve at the calibration time c for any value for α or σ, due to this, such parameters cannot be estimated by calibration (Kladívko and Rusý, 2023). For simplicity and since the scope of this study is to focus on the impact of pandemic risk on bond valuation, the value for the mean-reversion speed parameter will be assumed as $\alpha = 0.05$ (See table 5: Kladívko and Rusý, 2023) as this value fits the 95% confidence intervals based on both the likelihood ratio and the Wald test in Kladívo and Rusý's research that takes on a similar calibration framework.

Regarding the volatility parameter, as suggested by Lee (2021) I will use a piecewise constant volatility function. The volatility values were derived from the realized volatility in the EUR yields over the last 2 years. This approach assumes market stationarity and has considerable limitations as a predictor of future volatility, namely in the current EUR market which has been subject to pressure due to several factors, namely the COVID-19's pandemic impact on European economy leading to rising interest rates and record-high inflation, the current state of political uncertainty with European elections taking place in June 2024 and the uncertainty around the impact of artificial intelligence on regulations and interest rates (see: European Central Bank, n.d.; Deutschland.de, 2023; McCaffrey et al., 2023; Taylor, 2023). Despite this, due to convenience and accessibility to historical volatility data and a lack of access to implied volatilities data from swaptions prices, this approach will suffice for calibration purposes, in future research an implied volatility approach could be explored. Historical values for the chosen calibration instruments are plotted in Figure 3.

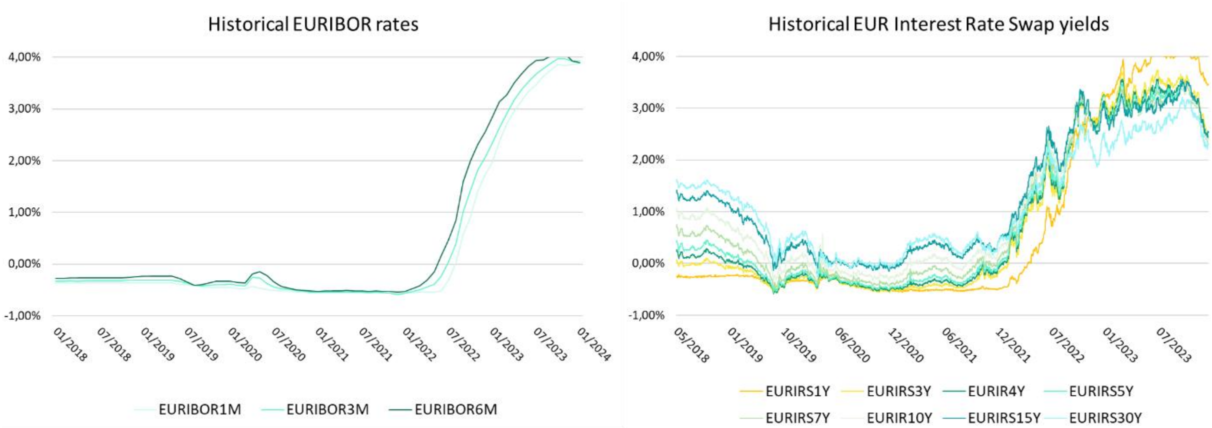

Figure 3: Historical values for Euribor 1M, 2M, 6M (on the left) and EURIRS 1Y, 3Y, 4Y, 5Y, 7Y, 10Y, 15Y, 30Y (on the right).

Please note that only the last two years of historical data were used to calibrate the model as these achieved more accurate predictions of future interest rates (according to mean-square error estimators) compared to the use of Euro interest swap data from the last 5 years. This is due to the impact of the COVID-19 pandemic on financial markets, as well as the recent armed conflict in Europe and other relevant political and economic frameworks.

The Hull-White model simulation consists of the computation of daily short rates for 10000 simulated interest rate paths within a 4-year period. Model parameters are described in table 3.

Table 3: Hull-White model simulation parameters

Hull-White model Parameters	
Calibration time c	31/12/2023
Day convention	Actual/360
Time step (in years)	1/360
Mean-reversion speed α	0,05
Maturity vector for volatility parameter σ (in years)	1/12, 3/12, 6/12, 1, 3, 4, 5, 7, 10, 15, 30
Volatility parameter vector derived at calibration time c (in years) derived from the previous 2 years of historical data.	0.01786, 0.01771, 0.01757, 0.01617, 0.01138, 0.01038, 0.00977, 0.0093, 0.00841, 0.00788, 0.00704
Maturity vector for spot rates r_c (in years)	1/12, 3/12, 6/12, 1, 3, 4, 5, 7, 10, 15, 30
Spot rates curve at calibration time c	0.03869, 0.03924, 0.03891, 0.03459, 0.02546, 0.02460, 0.02434, 0.02440, 0.02474, 0.02538, 0.02306
Number of simulated paths	10000
Simulated time	4 years

The simulated interest rate paths account for the 650 basis points spread, allowing for a more accurate estimate of discount factors when compared to a later adjustment on the mean discount factors of all 10000 simulations at each time step. Nevertheless, by subtracting the spread from the simulated interest rate paths, I compared the future interest rate predictions with the Euribor 6-months forward curve provided by Chatham Financial, n.d.). Taking into consideration that the Hull-White model simulation interest rate paths begin on 01/01/2024, this comparative analysis allows for a more comprehensive assessment of the model’s alignment with market expectations. The mean-square error computed in this analysis amounts to 4.39×10^{-06}, indicating a good match between predictions and the markets forward rate. Figure 4 provides visual representation of this comparison.

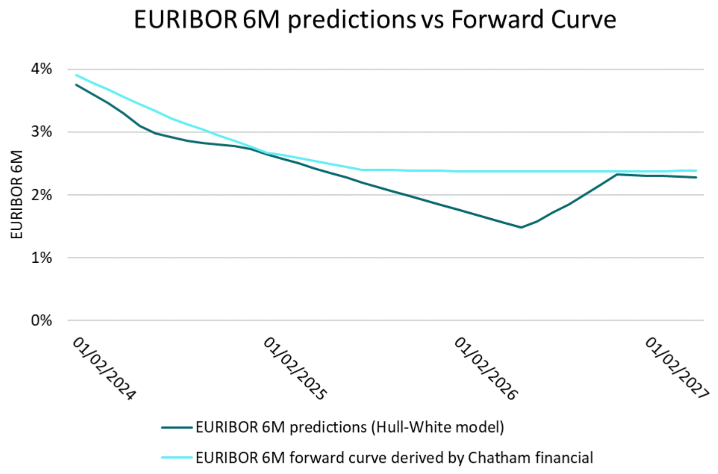

Figure 4: Hull-White model predictions plotted against the Euribor 6-months forward curve.

The Hull-White model implementation results are presented below. On the top-left corner of Figure 5 the 10000 simulated paths for the prices of zero-coupon bonds expressed as a percentage of their face value, on the top-right corner the simulated short rate paths, bellow on the left the respective discount factors and finally, on the bottom-right corner the simulated spot rate paths, that is, the yield to maturity of a default-free zero-coupon bond.

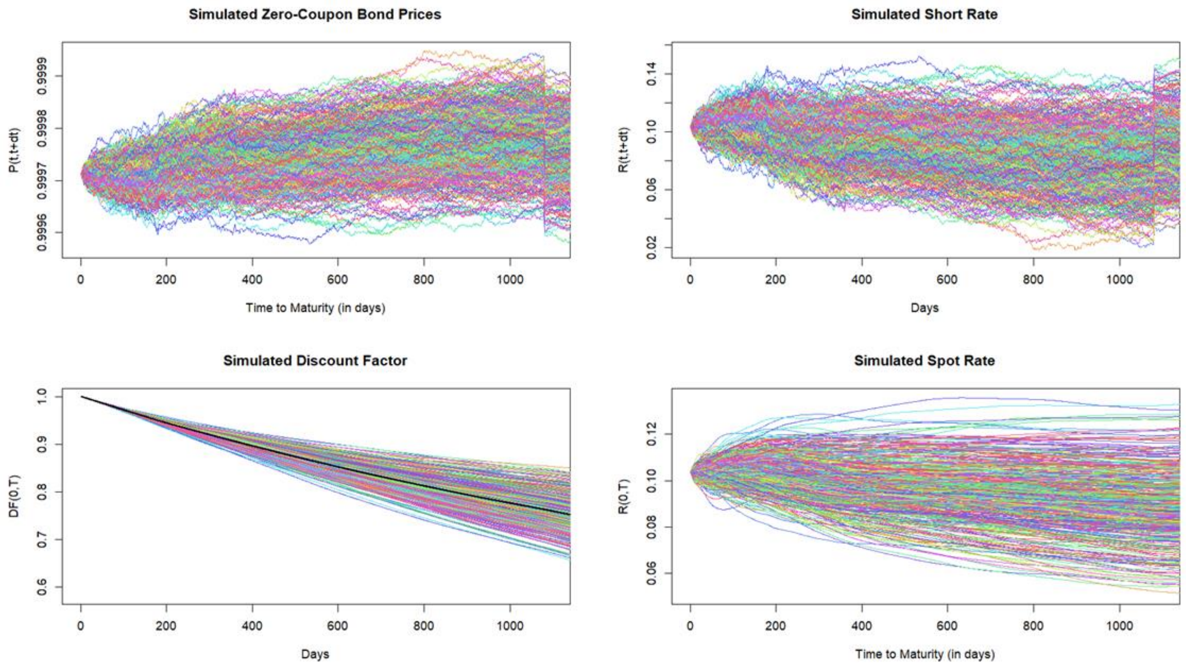

Figure 5: Hull-White model simulation results.

Note that around the three-year mark there is a disruption for all zero-coupon bond price and short rate paths, this is due to the decrease in realized volatility, used to calibrate the model, from the one-year maturity interest rate swap rate to the three-year maturity swap rate. This can be explained by an atypical yield curve reflecting markets expectation of decreased interest rates for longer maturities.

In fact, the Euro area yield curves currently drop around the 5th and 6th year maturities (see: European Central Bank, n.d.-a).

As suggested by Manathunga and Deng (2023), the mean of the daily short rates simulated withing each 6-month timeframe approximates the desired rate, Euribor 6-months + 650 basis points, for that given period. To reach the final interest rate predictions for future bond valuations I will also apply the mean to the average that was retrieved for each period for all 10000 simulations. After completing all iterations an average Euribor 6-months can be extracted for each semi-annual coupon payment date. Similarly, by computing the average discount factors across all 10000 simulations at each time step, the discount factors to compute the present value of each cash flow are determined.

As mentioned previously, I used the R code provided by Manathunga (2023) as a foundation for this empirical study. While implementing the code I identified and fixed several errors, such as an incorrect usage of discount factors as discount rates and additionally accounted for spread impact on discount factors (the authors had already accounted for this regarding coupon rates). Corrections are essential to ensure accuracy and reliability of the results presented in this thesis. Despite this, the original work of previous authors contributed to the initial development of the R code, serving as a valuable starting point for this research. The Hull-White model's predictions amount to an estimated present value of 197.568 million EUR, meaning that the proposed pandemic bond would be trading at a discount. Overall bond valuation results are shown in Table 4.

Table 4: Hull-White model results and bond valuation without pandemic risk adjustment.

Amounts in million EUR

Date	Time (in days)	Coupon rate	Coupon amount	Cash Flows	Discount Factors	Present Value of Cash Flows
01/01/24	0	–	–	–	–	–
01/07/24	182	9.519%	9.62474	9.62474	0.94887	9.13265
01/01/25	366	9.265%	9.47065	9.47065	0.90387	8.56021
01/07/25	547	8.814%	8.86253	8.86253	0.86284	7.64693
01/01/26	731	8.376%	8.56225	8.56225	0.82502	7.06402
01/07/26	912	8.017%	8.06141	8.06141	0.79123	6.37842
01/01/27	1096	8.824%	9.02005	209.02005	0.75967	158.78579
					Hull-White model Present Value	197.56802

4.3. COMPUTING THE PROBABILITY OF A PANDEMIC

Prior to the stochastic logistic growth model implementation to Germany COVID-19 data, the probability of occurrence of a pandemic must be set. Due to lack of data regarding pandemic occurrences, the probability of a pandemic of coronavirus is assumed as the probability of a pandemic in general. This is a simplifying assumption that can be revised in future studies as pandemic predictive methods evolve.

Note that Fan and Mamon (2023) examined pandemic occurrences over the last century, whereas I will focus on pandemic events within the past 25 years. The focus on the recent 25-year period stems from the fact that pandemic occurrences have followed shorter interpandemic periods in recent years, as depicted in Figure 6.

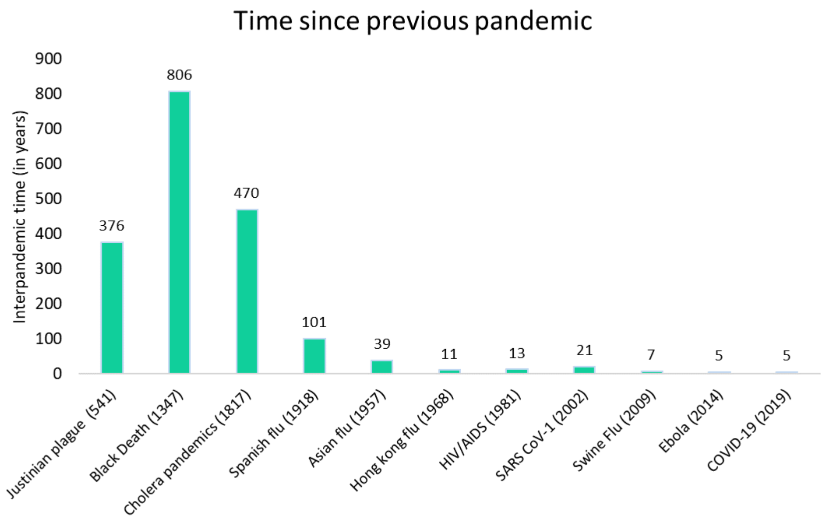

Figure 6: Interpandemic times represented as time since last registered pandemic for each global outbreak (see: Sampath et al., 2021)

The era of globalization has undoubtedly contributed to the spread of infectious diseases, the emphasis on the last 25 years ensures a focus on recent developments and their implications on this study.

From the Poisson modeling discussed in the methodology section, the estimated value for λ, considering the last 25 years of data, is 0.48. Thus, the probability of no pandemic during the three-year term of the proposed bond, $\mathbb{P}(H')$, is 0.6188 and the probability of a pandemic event during the bonds term, $\mathbb{P}(H)$, is 0.3812.

4.4. STOCHASTIC LOGISTIC GROWTH MODEL SIMULATION

Throughout this section I will present the results for different pandemic scenarios and their impact on bond valuation, as well as a sensitivity analysis of bond prices to the pandemic start date and to trigger activation probabilities. The bond will be valuated under the assumption that a pandemic has not yet been declared at issuance. Bond parameters are described in Section "4.1. Bond characteristics". The stochastic logistic growth model algorithm that served as a base for this study was first implemented by Manathunga (2023).

The historical COVID-19 data for Germany required for calibration of the stochastic logistic growth model was imported using the "covid19" R package (Guidiotti and Ardia, 2023). The data ranges from the 1st of March 2020, with 170 infected cases and 1 death, to the 31st of December 2022, with a total infected count of 37390541 and a death count of 165568. The thresholds for infected, $I(t)$, and deaths, $D(t)$, are set as 1% and $0{,}005\%$ of the German population on the 31st of December 2023 respectively, amounting to a threshold of 847000 cases and 4235 deaths (Statista, n.d.). This threshold approach would have meant that the bonds triggering conditions would have been activated on the 19th of March 2020 for the COVID-19 pandemic, on the 19th day of the historical dataset. The carrying capacities for infected, K_I, and deaths, K_D, were chosen as the maximum number of cases for each process taken from historical data. This approach is ultimately subjective and would essentially be a decision of the bond's issuer, but for the purposes of this study it is adequate.

The growth rates displayed in Figure 7 were derived from COVID-19 German historical data as follows:

$$g_I(t) = \frac{I(t) - I(t-1)}{I(t-1)} \qquad , \qquad g_D(t) = \frac{D(t) - D(t-1)}{D(t-1)}$$

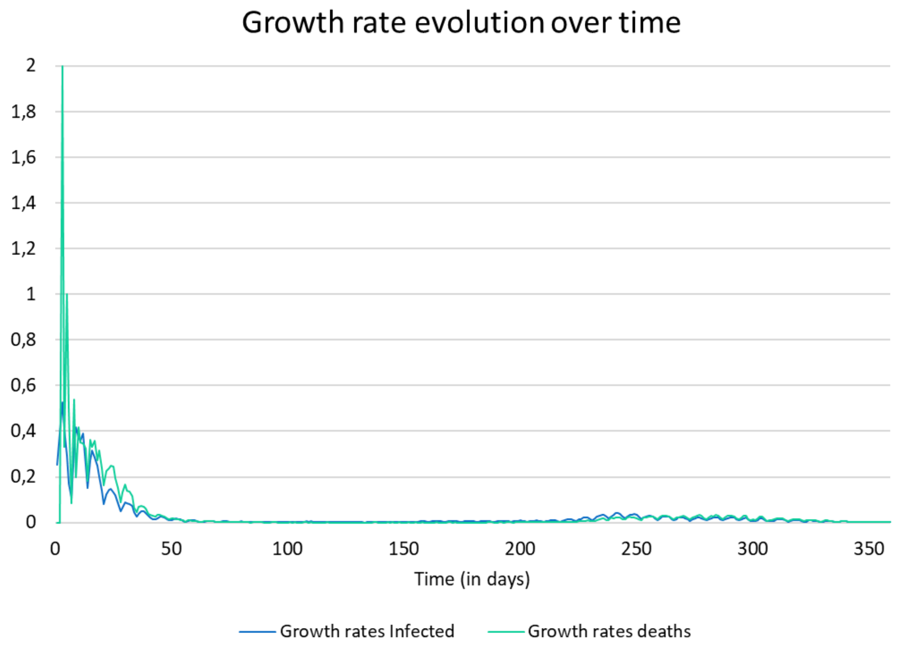

Figure 7: Growth rates for infected and deaths in Germany from COVID-19 historical data.

4.4.1. Model Calibration and growth rate scenario impact on bond valuation

In this section I evaluate three pandemic scenarios and assess their impact on bond valuation. In Scenario I the growth rate g_I is calculated as the average growth rate for the first week of available data, Scenario II expands the range of data to the first two weeks and Scenario III encompasses the average growth rate over the initial thirty-day period of historical data. The standard deviation for growth rates follows the same logic across all three scenarios. Due to numerical implementation issues the growth rates and respective standard deviations for deaths must be set to the same values as for infected. This issue was first reported by Manathunga and Deng (2023), who noticed that when the two rates differed there would be a significant and unnatural delay between the infection and deaths curves, as it was longer than the average infectious period. Ideally, each process is driven by their own growth rates and standard deviations and this methodological gap should be addressed in later research.

The previous author's analysis solely considered trigger activation for a pandemic that began shortly after the bond's issuance, where triggering events predominantly manifested within the initial months of the bond's term. Manathunga and Deng's (2023) simulation amounted to a higher percentage of coupon bond payment loss, as all future payments since trigger activation are lost. However, this approach does not account for the occurrence of lesser impacts. In this study I aim for a more realistic approach by accounting for the possibility of a pandemic starting later relative to the bonds term. For the initial three scenarios, the timeline of the pandemic relative to the bond term was randomly generated in R following an assigned probability distribution. As the COVID-19 pandemic is a recent event, the likelihood of a new pandemic occurring within the first year was set as 0.2, within the second year as 0.3 and within the third year at 0.5. It is important to note that these probabilities sum up to 1, as the simulation presumes the occurrence of a pandemic during the bonds' term, and were chosen for illustrative purposes, thus may not precisely reflect the actual probabilities of a new pandemic occurring under each timeline. The next section further explores the impact of the timeline of the pandemic on bond valuation.

Scenario parameters are summarized in Table 5, please note that bond price is expressed in million EUR.

Table 5: Stochastic Logistic Growth scenarios I, II and III parameters and results

	Scenario I	**Scenario II**	**Scenario III**
Number of Simulations	10000	10000	10000
$\mathbb{P}(H)$	0.3812	0.3812	0.3812
K_I	37390541	37390541	37390541
K_D	165568	165568	165568
$I(0)$	150	150	150
$D(0)$	1	1	1
g_I , g_D	0.3084	0.3158	0.2308
σ_I , σ_D	0.1459	0.1181	0.1281
$\rho_{I,D}$	0.65	0.65	0.65
θ_I	847000	847000	847000
θ_D	4235	4235	4235

The correlation coefficient between infected, $I(t)$, and deaths, $D(t)$, was set as 0.65. This value reflects an understanding of the potential correlation between these processes, it is important to note that this decision was not directly informed by empirical research or established literature. It assumed, from historical data analysis, that there exists some level of correlation between infections and deaths. I recognize the complexity and variability inherent to such relationships, and the need for further analysis under different contexts.

The graphs displayed in Figure 8 depict the trajectories of the seven-day moving average for daily new infections, $MA_I(T)$, and deaths, $MA_D(T)$, for randomly selected simulated paths. The selective approach to plotting saves time, as plotting is time consuming, while also enhancing visual appeal and clarity in graph analysis, as only 100 simulated paths were selected. Additionally, threshold lines indicating trigger activation have been incorporated in the graphs. These lines denote the points at which trigger conditions are satisfied, enhancing the visual representation of these critical moments for bond valuation.

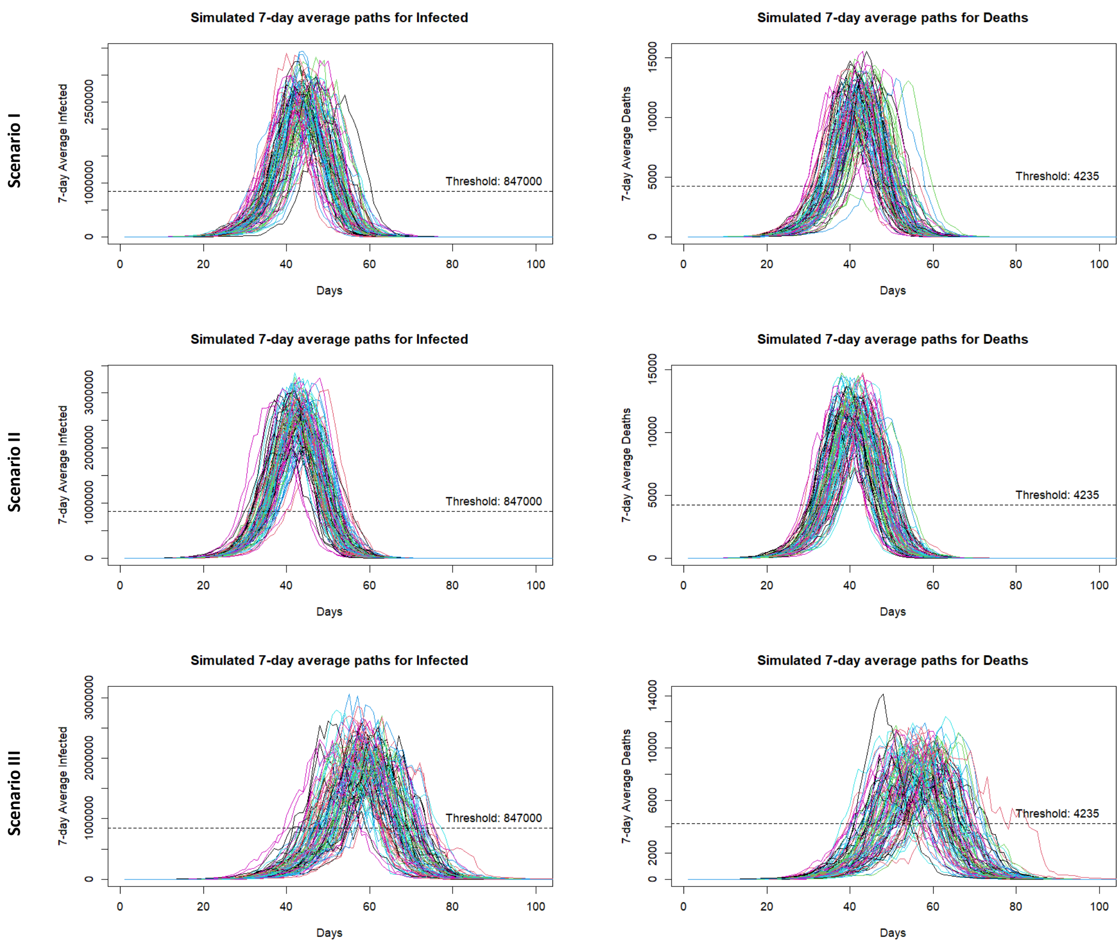

Figure 8: Seven-day average trajectories for Infected, I(t), and deaths, D(t), simulated paths.

The six plots are distributed as infected and deaths by column, with each scenario represented in each row. Scenario II exhibits similarities to Scenario I, with closely aligned growth rates of around 31%. Despite their similarities, Scenario II leads to slightly earlier triggers across overall simulations. Furthermore, Scenario I is associated with a higher volatility compared to Scenario II, which becomes evident in the broader spread of paths over time. Conversely, Scenario III, characterized by a lower growth rate, requires a longer duration to meet triggering conditions. Despite having a lower volatility parameter than Scenario I, Scenario III appears to be more volatile, with paths noticeably spread out. This may be attributed to the higher discrepancy between the growth rate and its standard deviation in comparison to Scenario I. Scenario III leads to considerably later trigger activation times, ranging from around the 37th day since the beginning of the pandemic, to the 60th day, while the other two scenarios lead to triggering conditions activation from around the 25th to the 45th days. Table 6 presents model results under each scenario.

Table 6: Stochastic Logistic growth simulation and bond valuation results for scenarios I, II and III.

	Scenario I	**Scenario II**	**Scenario III**
g_I , g_D	0.3084	0.3158	0.2308
σ_I , σ_D	0.1459	0.1181	0.1281
$\mathbb{P}(C)$	0.3804	0.3808	0.3795
Bond Price	137.1599	134.6137	132.2101
Bond price as a % of Face Value	0.6858	0.6731	0.6611

From Table 6, several conclusions can be drawn. The analysis reveals a decrease in the bond's price from 68.58% of its face value to 66.11% as the time frame for growth rate calibration increases. As previously mentioned, growth rates for scenarios I and II are very similar, around 31%, and higher than the one used for scenario III which is around 23%. Conversely, scenarios II and III are linked by a similar growth rate standard deviation of around 12%, while scenario I presents a higher value of around 15%. These values, computed from historical data, are corroborated by Figure 7, where it is noticeable that peak growth rates of around 200% occur during the first week, followed by an exponential decrease that converges around the 50th day.

As the simulation relies on a stochastic logistic growth model with a constant growth rate and standard deviation, a longer timeframe for model calibration leads to a lower average growth rate for infected cases. A longer timeframe leads to a longer period to trigger activation. Therefore, the longer calibration window correlates with lower bond valuations. Notice that scenario II presents a higher trigger activation probability than scenario I, but results in a lower bond price due to earlier triggers and the loss of all future coupon payments. Therefore, trigger activation timing becomes more critical than the trigger activation probability itself.

4.4.2. Pandemic timeline relative to bonds term and its impact on bond prices

Understanding the relationship between the day a pandemic begins and bond terms is crucial for evaluating pandemic bonds as these instruments account for potential future coupon and principal loss following a triggering event. For this purpose, I generated a vector representing each possible day, since the bonds issuance until maturity, for the pandemic to begin. Subsequently, I simulated 10000 pandemic paths employing a stochastic logistic growth model starting at time 0 relative to the pandemic's start date. By evaluating trigger times within this model and adding these times to each of the 1094 days generated as possible pandemic start dates, I determined the days it would take for each pandemic to activate triggering conditions, given each start date. With this information, I performed bond valuation, triggered paths result in the loss of all future coupon and principal payments and paths without trigger activation result in the realization of full bond payout structure. The average bond prices across the 10000 simulated pandemic paths resulted in the predicted bond price for each start date.

The parameters used for the stochastic logistic growth model simulation are presented in table 7.

Table 7: Stochastic logistic growth model parameters for Scenario IV.

	Scenario IV
Number of Simulations	10000
$\mathbb{P}(H)$	0.3812
K_I	37390541
K_D	165568
$I(0)$	150
$D(0)$	1
g_I , g_D	0.2850
σ_I , σ_D	0.1307
$\rho_{I,D}$	0.65
θ_I	847000
θ_D	4235

Most parameters match the selection made for Scenarios I, II and III, except for the growth rates and respective standard deviations, which were computed as the mean of the parameter choices for the three previous scenarios. By computing the mean of the parameter choices for these scenarios, I aim at providing a comprehensive representation of pandemic dynamics, encompassing elements from previous simulations. This approach also allows for comparability with each individual scenario, thus leading to meaningful insights into the relative impact of the pandemic timing on bond prices. As a result of a total of 10.96 million simulations, a mean bond price was evaluated as 133.2993 million EUR, associated with a trigger activation probability of 0.3809. Overall simulation results are presented in Table 8.

Table 8: Scenario IV simulation results.

	Scenario IV
$\mathbb{P}(C)$	0.3809
Bond Price	133.2993
Bond Price as a % of Face Value	66.6497%

Figure 9 displays the corresponding bond prices against the start date of the pandemic.

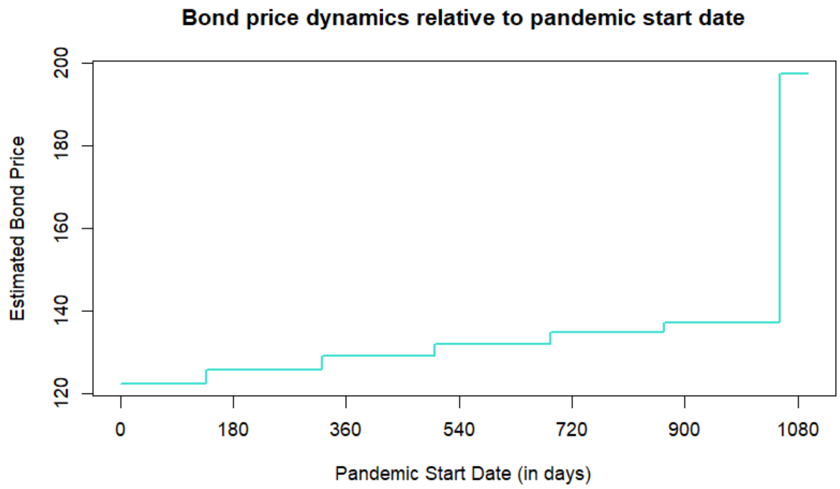

Figure 9: Bond price dynamics against pandemic start date.

As expected, the graph takes on a staircase-like pattern indicating that trigger activations occurring between coupon payment dates result in consistent bond prices over certain intervals. The segments for which bond prices remain constant reflect the inherent structure of pandemic bonds, namely the proposed bond, as these segments seem to be structured as semi-annual periods, matching the coupon payment dates. Conversely, leaps in bond prices, visible through the vertical sections in the graph, highlight fluctuations in bond prices associated with trigger activation events occurring on coupon payment dates. Note that leaps in bond prices do not align with coupon payment dates as prices are plotted against the beginning of the pandemic and there is a period where the pandemic has already begun but triggering conditions cannot be fulfilled prior to the next coupon payment, resulting in a price increase. Notice that this discrepancy aligns with the average period between the pandemics inception and the date at which triggering events occurred visible in the seven-day average simulation results for scenarios I, II and III in Figure 8.

Another relevant conclusion can be drawn from the graph, as a notable pattern emerges. The increments in bond prices become progressively smaller as the pandemic start date reaches maturity, indicating a decay in the discount amount associated with these bonds. A possible explanation for this phenomenon is the impact of investor perception of risk, as there is heightened uncertainty around bond payouts for pandemics triggered at latter times. Furthermore, accounting for an expected decrease in the floating rate as time progresses, visible through the Hull-Whites model predictions, coupon payment amounts tend to decrease over time. The only exception is the leap in bond prices closer to maturity, which is visibly the largest one, occurring just before the 1080th day of the bonds term, meaning that for pandemics beginning after this date, triggering conditions could not be met prior to the last coupon and principal payment at maturity.

Additionally, note that the bond trades at a higher discount given pandemic inception dates in earlier times during the bonds term, when compared to subsequent dates, which aligns with the bond's payout structure of potential future coupon payment loss.

This analysis provides relevant insights into the dynamics between pandemic start dates, trigger activation timing and bond valuation, contributing for risk assessment and investment decision-making in pandemic bond markets.

4.4.3. Bond Price sensitivity analysis: Wang transform

The final pandemic scenario presented in this study aims at clarifying the impact of trigger activation probabilities on bond valuation, while preserving the pandemics' inception date approach adopted in Scenario IV. Scenario V comprises 5 sub-scenarios, each corresponding to a different adjustment of trigger activation probabilities through the Wang transform, as to reflect the market's level of risk aversion or optimism regarding the occurrence of triggers and their impact on the bond's payouts.

Table 9 describes scenario parameters, translating each choice to a level of market price of risk and investor sentiment.

Table 9: Wang transform adjustment: Scenario V parameters and description.

Scenario	λ	Market price of risk	Investor sentiment	Bond Price Dynamics
$\boldsymbol{V_{\lambda=0.01}}$	0.01	Very low	Low risk aversion or high optimism	Skewed towards higher values
$\boldsymbol{V_{\lambda=0.1}}$	0.1	Low	Low-moderate risk aversion or moderate optimism	Less skewed towards higher values
$\boldsymbol{V_{\lambda=0.5}}$	0.5	Moderate	Moderate risk aversion or balanced views	Evenly distributed
$\boldsymbol{V_{\lambda=1.0}}$	1.0	Neutral	Neutral risk aversion or uncertainty	Evenly distributed
$\boldsymbol{V_{\lambda=5}}$	5.0	High	High risk aversion or pessimism	Skewed towards lower values

Figure 10 displays the fair value for the pandemic bond according to investors' expectations and the market price of risk adjustment scenario.

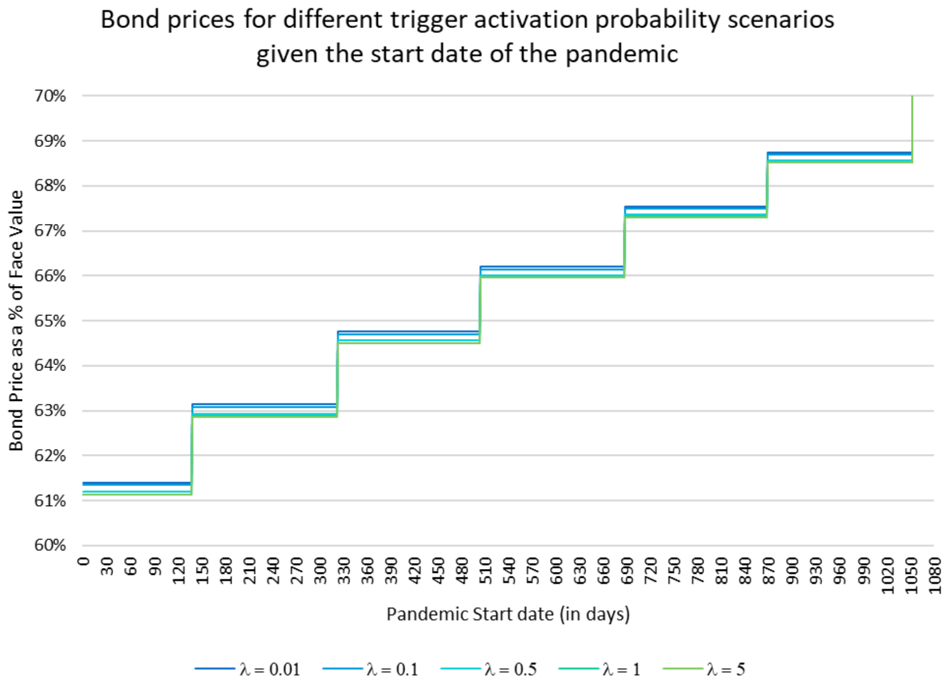

Figure 10: Bond valuation results for different λ scenarios and pandemic inception dates.

Please note that for pandemics happening shortly after the 1050th day since bond issuance, the bonds' fair price is the result of a full payout structure, as pandemics starting after this date will not activate triggering conditions before bond maturity. Due to this, Figure 10 focuses on the pricing dynamics that account for a loss of redemption amount. Moreover, the graph illustrates that a higher adjustment in the market price of risk leads to bond valuations trading at a greater discount compared to a lower adjustment scenario. This reflects investors' perception of heightened risk.

Figure 11 illustrates price disparity under the higher market sentiment scenarios, comparing these to the lowest adjustment scenario. Thus, providing insights into investors' reactions to pandemic risk and trigger activation probabilities.

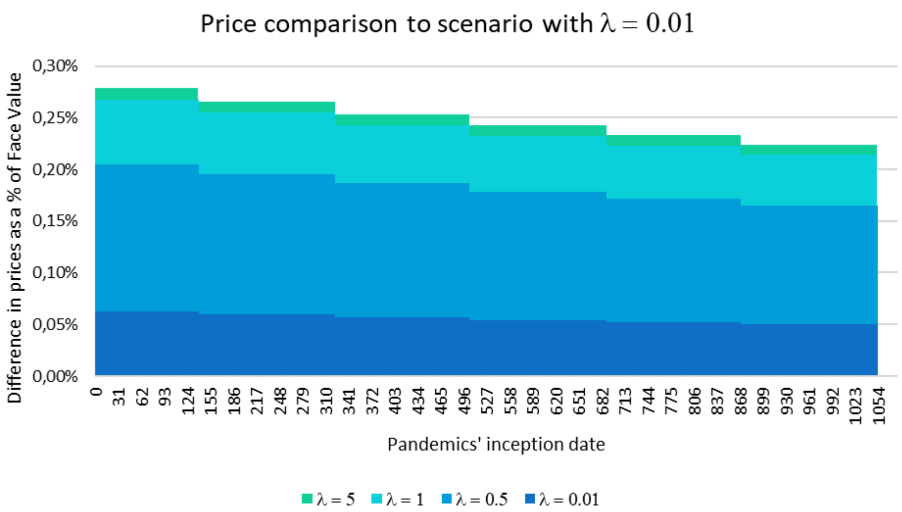

Figure 11: Price discrepancy between scenarios.

The impact of investors' risk profile toward pandemic risk, simulated through varying λ values, is particularly pronounced for scenarios where the potential pandemic is anticipated to begin within the first 130 days of the bond's term. In these instances, a more notable discrepancy in bond valuations is observed for earlier pandemic inception dates. The highest discrepancy in bond prices corresponds to a difference of 0.2784% of the bond's face value between scenarios representing very low and high market risk. Table 10 aims to elucidate the extent of price disparity under different market sentiment scenarios.

Table 10: Price difference amongst scenarios for pandemics starting in the first 130 days of the bonds term.

	Price difference (as a % of Face Value) in comparison to scenario $V_{\lambda=0.01}$
$V_{\lambda=0.1}$	0,0621%
$V_{\lambda=0.5}$	0,2048%
$V_{\lambda=1.0}$	0,2669%
$V_{\lambda=5}$	0,2784%

By calibrating lambda to reflect different levels of risk aversion or optimism in the market, I aim to elucidate how investor sentiment influences trigger event probabilities and, consequently, bond valuation dynamics.

5. CONCLUSIONS AND FUTURE WORKS

In 2017, the World Bank launched the innovative pandemic bonds, aiming to shift pandemic risk from developing countries to global financial markets. Similarly to CAT bonds, these insurance linked securities featured predetermined triggering conditions and investors faced potential future coupon payment and principal losses should these be met. As a result, bond proceeds were directed to cover issuer losses. However, the COVID-19 pandemic revealed shortcomings for these bonds due to the complexity of triggering conditions.

As pandemics show an increasing frequency, research on effective pandemic risk management strategies plays a crucial role in strengthening financial markets and insurance industry resilience to such events. Furthermore, with an issuance surge in 2023, the catastrophe bond market has shown growth over the years, highlighting investors' appetite for risks associated with extreme events.

The present study seeks to extend existing pandemic bond pricing literature, namely the Hull-White stochastic logistic growth pricing framework, by incorporating price scenarios dependent on a pandemic's inception date relative to the bonds term and performing price sensitivity analysis to trigger activation likelihood through the Wang transform. Ultimately reflecting market risk preferences on the pricing and assessment of triggering events in pandemic bond valuation.

This framework allows for a clearer view of expected bond prices according to different scenarios, empowering investors to make more informed decisions. The employed methodology is relatively straightforward, facilitating comprehension for investors with a varying level of expertise. However, its simplifying assumptions may compromise accuracy.

The Hull-White model offers advantages such as the calibration to current interest rates, due to its arbitrage-free nature, and accommodation of negative interest rates, which have been observed in the past. While it poses a more comprehensive approach when compared to constant volatility, the use of a piecewise constant volatility function may not fully capture the dynamic nature of financial markets. Building on this, volatility values for numerical implementation were derived from realized volatility, rather than implied volatilities, assuming market stationarity, which may not hold true. Additionally, note that the model relies on financial markets independence from pandemic events, while the COVID-19 pandemic established a correlation between the two.

The stochastic logistic growth model has shown accuracy in infected and death process prediction for pandemics like COVID-19, however the assumption of a fixed correlation between the two processes may oversimplify real-world dynamics. A nonautonomous approach to this correlation would lead to more accurate depictions. The incorporation of environmental noise poses an advantage when modelling the number of infected and dead, as it allows for a more realistic approach to the complexities of the pandemic event. Overall, the model's reliance on historical data for model calibration may introduce biases and inaccuracies.

Previous authors relied on the assumption that if a pandemic were to occur during the bonds term it would be shortly after issuance, relying only on the time it would take for the pandemic to gain form and activate triggering conditions. In response to the identified gaps in existing literature, I present a framework that accounts for the impact of the pandemic's inception date in bond valuation.

Future research could address the numerical implementation of a nonautonomous stochastic logistic growth model integrated with a more accurate depiction of the probability distribution for a pandemic's inception date across the bond's term. While this study primarily focused on price sensitivity given a pandemic's starting date, a more comprehensive approach that accounts for the stochastic nature of pandemic occurrences could provide a more realistic representation of real-life pandemics and their distributions.

The emerging field of pandemic bond pricing demands a multidisciplinary approach. Future studies could explore the integration of knowledge from risk management, economics, and epidemiology to refine pricing models. Collaboration from diverse fields holds the potential to advance our understanding of pandemic risk and improve the efficacy of pandemic bond pricing mechanisms in the future.

BIBLIOGRAPHIC REFERENCES

After COVID-19: The future of pandemic bonds. (n.d.). Retrieved June 6, 2023, from https://www.ft.com/partnercontent/calvert/after-covid-19-the-future-of-pandemic-bonds.html

Artemis. (2024). *Bond & ILS Market Report Q4 2023 Catastrophe*. Retrieved February 3, 2024, from https://www.artemis.bm/

Braun, A. (2012). Determinants of the cat bond spread at issuance. *Zeitschrift Fur Die Gesamte Versicherungswissenschaft*, *101*(5), 721–736. https://doi.org/10.1007/s12297-012-0221-3

Bühlmann, H. (1980). ETH Library An Economic Premium Principle. *Astin Bulletin*, *11*(1), 52–60. https://doi.org/10.3929/ethz-b-000422521

Burnecki, K., & Kukla, G. (2003). Pricing of zero-coupon and coupon cat bonds. *Applicationes Mathematicae*, *30*(3), 315–324. https://doi.org/10.4064/am30-3-6

Chatham Financial. (n.d.). Retrieved February 1, 2024, from https://www.chathamfinancial.com/

Chen, F. Y., Yang, S. S., & Huang, H. C. (2022). Modeling pandemic mortality risk and its application to mortality-linked security pricing. *Insurance: Mathematics and Economics*, *106*, 341–363. https://doi.org/10.1016/j.insmatheco.2022.06.002

Cox, J. C., Ingersoll, J. E., & Ross, S. A. (1985). A Theory of the Term Structure of Interest Rates. In *Econometrica*, 53(2), 385–407. https://doi.org/10.2307/1911242

Cox, S. H., & Pedersen, H. W. (2000). Catastrophe risk bonds. *North American Actuarial Journal*, *4*(4), 56–82. https://doi.org/10.1080/10920277.2000.10595938

Deng, G., Liu, S., Li, L., Deng, C., & Yu, W. (2020). Research on the Pricing of Global Drought Catastrophe Bonds. *Mathematical Problems in Engineering*, *2020*. Article ID 3898191. https://doi.org/10.1155/2020/3898191

Denuit, M., Devolder, P., & Goderniaux, A.-C. (2007). Securitization of Longevity Risk: Pricing Survivor Bonds with Wang Transform in the Lee-Carter Framework. In *Source: The Journal of Risk and Insurance,* 74(1). Retrieved from http://www.jstor.org/stable/4138426

Deutschland.de. (2023, December 18). *Landmark European elections in 2024*. Retrieved January 12, 2024, from https://www.deutschland.de/en/topic/politics/european-elections-in-germany-in-2024

Egami, M., & Young, V. R. (2007). *Indifference Prices of Structured Catastrophe (CAT) Bonds*. Insurance Mathematics and Economics, 42(2), 771–778. https://doi.org/10.1016/j.insmatheco.2007.08.004

European Insurance and Occupational Pensions Authority. (2021). The insurability of business interruption risk in light of pandemics. Publications Office. https://data.europa.eu/doi/10.2854/293053

EURIBOR.EU. (n.d.). *Historical Euribor rates and graphs*. Retrieved February 12, 2024, from https://euribor.eu/historical-euribor-rates-and-graphs/

European Central Bank. (n.d.-a). *Euro area yield curves*. Retrieved February 13, 2024, from https://www.ecb.europa.eu/stats/financial_markets_and_interest_rates/euro_area_yield_curves/html/index.en.html

European Central Bank. (n.d.-b). *Financial Stability Review, November 2023*. Retrieved February 1, 2024, from https://www.ecb.europa.eu/pub/financial-stability/fsr/html/ecb.fsr202311~bfe9d7c565.en.html

Fan, W., & Mamon, R. (2023). A Hybridized Stochastic SIR-Vasiček Model in Evaluating a Pandemic Emergency Financing Facility. *IEEE Transactions on Computational Social Systems*, *10*(3), 1105–1114. https://doi.org/10.1109/TCSS.2021.3131260

Golec, J., & Sathananthan, S. (2003). Stability Analysis of a Stochastic Logistic Model. *Mathematical and Computer Modelling,* 38(5–6), 585-593. https://doi.org/10.1016/S0895-7177(03)90029-XGuidiotti, E., & Ardia, D. (2023).

Guidotti, E., & Ardia, D. (2023). COVID19: R Interface to COVID-19 Data Hub. Retrieved from https://cran.r-project.org/web/packages/COVID19/index.html

Härdle, W. K., & Cabrera, B. L. (2010). Calibrating CAT bonds for Mexican earthquakes. *Journal of Risk and Insurance*, *77*(3), 625–650. https://doi.org/10.1111/j.1539-6975.2010.01355.x

Hartwig, R., Niehaus, G., & Qiu, J. (2020). Insurance for economic losses caused by pandemics. *Geneva Risk Insur Rev*, *45*, 134–170. https://doi.org/10.1057/s10713-020-00055-y

Holzheu, T., & Lechner, R. (2023, December 14). Surge in catastrophe bond issuance stabilises transfer of mounting peak risks. *Swiss Re Institute*, Retrieved January 3 2024 https://www.swissre.com/institute/research/sigma-research/Economic-Insights/catastrophe-bond-issuance.html

Huang, S., Seng Tan, K., Zhang, J., & Zhu, W. (2021). Epidemic Financing Facilities: Pandemic Bonds and Endemic Swaps. *North American Actuarial Journal*. Advance online publication. https://doi.org/10.1080/10920277.2023.2256818

Hull, J., & White, A. (1990). Pricing Interest-Rate-Derivative Securities. *The Review of Financial Studies* 3(4), 573-592. https://www.jstor.org/stable/2962116

Hull, J., & White, A. (1994). Hull_1994_Numerical procedures for implementing Term Structure Models I. *The Journal of Derivatives*, *2*(1), 7–16. https://doi.org/10.3905/jod.1994.407902

Investing.com. (n.d.). *EUR IRS Rates*. (N.d.). Retrieved February 1, 2024, from https://www.investing.com/search/?q=EURIRS

Jarrow, R. A. (2009). Credit Risk Models. *Annual Review of Financial Economics*, *1*, 37–68. https://doi.org/10.1146/annurev.financial.050808.114300

Jarrow, R. A. (2010). A simple robust model for Cat bond valuation. *Finance Research Letters*, *7*(2), 72–79. https://doi.org/10.1016/j.frl.2010.02.005

Khodabin, M., Maleknejad, K., Rostami, M., & Nouri, M. (2012). Interpolation solution in generalized stochastic exponential population growth model. *Applied Mathematical Modelling*, *36*(3), 1023–1033. https://doi.org/10.1016/j.apm.2011.07.061

Kijima, M., & Muromachi, Y. (2008). Extensions of the Wang transform for the pricing of insurance and financial risks. *Insurance Mathematics and Economics*, *42*(3), 887-896. https://doi.org/10.1016/j.insmatheco.2007.10.010

Kladívko, K., & Rusý, T. (2023). Maximum likelihood estimation of the Hull–White model. *Journal of Empirical Finance*, *70*, 227–247. https://doi.org/10.1016/j.jempfin.2022.12.002

Labuschagne, C. C. A., & Offwood, T. M. (2013). Pricing exotic options using the Wang transform. *North American Journal of Economics and Finance*, *25*, 139–150. https://doi.org/10.1016/j.najef.2012.06.008

Lee, J. P., & Yu, M. T. (2002). Pricing default-risky CAT bonds with moral hazard and basis risk. *Journal of Risk and Insurance*, *69*(1), 25–44. https://doi.org/10.1111/1539-6975.00003

Lee, S. (2021). Hull-White 1-factor model using R code. *R Bloggers*. Retrieved December 12, 2023, from https://www.r-bloggers.com/2021/06/hull-white-1-factor-model-using-r-code/

Li, H., Liu, H., Tang, Q., & Yuan, Z. (2023). Pricing extreme mortality risk in the wake of the COVID-19 pandemic. *Insurance: Mathematics and Economics*, *108*, 84–106. https://doi.org/10.1016/j.insmatheco.2022.11.002

Liu, M., & Wang, K. (2013). A note on stability of stochastic logistic equation. *Applied Mathematics Letters*, *26*(6), 601–606. https://doi.org/10.1016/j.aml.2012.12.015

Ma, Z. G., & Ma, C. Q. (2013). Pricing catastrophe risk bonds: A mixed approximation method. *Insurance: Mathematics and Economics*, *52*(2), 243–254. https://doi.org/10.1016/j.insmatheco.2012.12.007

Manathunga, V. (2023). Pricing-Pandemic-Bonds-under-Stochastic-Logistic-Growth-Model. *Github*. Retrieved December 12, 2023, from https://github.com/cvajira/Pricing-Pandemic-Bonds-under-Stochastic-Logistic-Growth-Model/blob/main/README.md

Manathunga, V., & Deng, L. (2023). Pricing Pandemic Bonds under Hull–White & Stochastic Logistic Growth Model. *Risks*, *11*(9). https://doi.org/10.3390/risks11090155

McCaffrey, C. R., Jones, O., & Krumbmüller, F. (2023). 2024 Geostrategic Outlook How to thrive amid ongoing geopolitical complexity. *EY*. Retrieved January 16, 2024, from https://assets.ey.com/content/dam/ey-sites/ey-com/en_gl/topics/geostrategy/ey-2024-geostrategic-outlook-report.pdf

Otunuga, O. M., & Otunuga, O. (2022). Stochastic Modeling and Forecasting of Covid-19 Deaths: Analysis for the Fifty States in the United States. *Acta Biotheoretica*, *70*(4). https://doi.org/10.1007/s10441-022-09449-z

Piantedosi, I. (2020). *CAT bonds and Pandemic bonds: the World Bank unique experience and the new challenge for the Insurance Industry*. (Master's thesis). Luiss Guido Carli. Retrieved November 22, 2023, from https://tesi.luiss.it/id/eprint/29369

Polacek, A. (2018). Catastrophe bonds: A primer and retrospective. *Chicago Fed Letter*, (No. 405). https://doi.org/10.21033/cfl-2018-405

R Core Team. (2023). _*R: A Language and Environment for Statistical Computing*_. R Foundation for Statistical Computing, Vienna, Austria. https://www.R-project.org/

Sampath, S., Khedr, A., Qamar, S., et al. (2021, September 20). Pandemics Throughout the History. *Cureus*, *13*(9). https://doi.org/10.7759/cureus.18136

Shen, C. Y. (2020). Logistic growth modelling of COVID-19 proliferation in China and its international implications. *International Journal of Infectious Diseases*, *96*, 582–589. https://doi.org/10.1016/j.ijid.2020.04.085

Statista. (n.d.). *Development of population numbers in Germany from 1990 to 2023*. Retrieved January 16, 2024, from https://www.statista.com/statistics/672608/development-population-numbers-germany/#:~:text=This%20statistic%20shows%20the%20development%20of%20population%20numbers,of%20that%20year%2C%20amounted%20to%2084.7%20million%20people.

Taylor, D. (2023, July 22). *AI Predictions: Future Impact On Exchange Rates, Equities, Interest Rates And Commodities*. [Blog post]. *Exchange Rates*. Retrieved February 13, 2024, from https://www.exchangerates.org.uk/news/38725/2023-07-22-artificial-intelligence-predictions-future-ai-impact-on-exchange-rates-equities-interest-rates-and-commodities.html

Triambak, S., Mahapatra, D. P., Mallick, N., & Sahoo, R. (2021). A new logistic growth model applied to COVID-19 fatality data. *Epidemics*, *37*. https://doi.org/10.1016/j.epidem.2021.100515

Vasicek, O. (1977). An equilibrium characterization of the term structure. In *Journal of Financial Economics*, *5*, 177-188. https://doi.org/10.1016/0304-405X(77)90016-2

Vaugirard, V. (2004). A canonical first passage time model to pricing nature−linked bonds. In *Economics Bulletin*, 7(2), 1-7. Retrieved January 18 2024 from http://www.economicsbulletin.com/2004/volume7/EB-04G10002A.pdf

Vaugirard, V. E. (2003a). Pricing catastrophe bonds by an arbitrage approach. *The Quarterly Review of Economics and Finance*, *43*(1), 119–132. https://doi.org/10.1016/S1062-9769(02)00158-8

Vaugirard, V. E. (2003b). Valuing catastrophe bonds by Monte Carlo simulations. *Applied Mathematical Finance*, *10*(1), 75–90. https://doi.org/10.1080/1350486032000079741

Vogels, M., Zoeckler, R., Stasiw, D. M., et al. (1975). P. F. Verhulst's "notice sur la loi que la populations suit dans son accroissement" from correspondence mathematique et physique. Ghent, vol. X, 1838. *Journal of Biological Physics*, *3*(4), 183–192. https://doi.org/10.1007/BF02309004

Wang, C. W., Yang, S. S., & Huang, H. C. (2015). Modeling multi-country mortality dependence and its application in pricing survivor index swaps-A dynamic copula approach. *Insurance: Mathematics and Economics*, *63*, 30–39. https://doi.org/10.1016/j.insmatheco.2015.03.019

Wang, S. S. (2000). A Class of Distortion Operators for Pricing Financial and Insurance Risks. *The Journal of Risk and Insurance*, *67*(1), 15–36.

World Bank. (2017a). *Pandemic Emergency Financing Facility (PEF) Framework: Prospectus Supplement* Dated June 28, 2017. Retrieved July 17, 2023, from https://thedocs.worldbank.org/en/doc/f355aa56988e258a350942240872e3c5-0240012017/.

World Bank. (2017b). *Pandemic Emergency Financing Facility_ Frequently Asked Questions*.

World Bank. (2017c). *World Bank Launches First-Ever Pandemic Bonds to Support $500 Million Pandemic Emergency Financing Facility*. [Press release]. Retrieved June 17, 2023,from https://www.worldbank.org/en/news/press-release/2017/06/28/world-bank-launches-first-ever-pandemic-bonds-to-support-500-million-pandemic-emergency-financing-facility

Young, V. R. (2004). Pricing in an incomplete market with an affine term structure. *Mathematical Finance*, *14*(3), 359–381. https://doi.org/10.1111/j.0960-1627.2004.00195.x

Zheng, X., & Mamon, R. (2023). Assessment of a pandemic emergency financing facility. *Progress in Disaster Science*, *18*. https://doi.org/10.1016/j.pdisas.2023.100281